Gene Therapy (2006) 13, 906–916

www.nature.com/gt

ORIGINAL ARTICLE

Transthoracic direct current shock facilitates intramyocardial transfection of naked plasmid DNA infused via coronary vessels in canines

Y Iida[1,2,6], Y Oda[1,6], S Nakamori[1,2,6], S Tsunoda[1,2,6], T Kishida[2,3], S Gojo[4], M Shin-Ya[2], H Asada[2], J Imanishi[2], T Yoshikawa[5], H Matsubara[1] and O Mazda[2]

[1]*Department of Molecular Cardiology and Vascular Regenerative Medicine, Kyoto Prefectural University of Medicine, Kyoto, Japan;* [2]*Department of Microbiology, Kyoto Prefectural University of Medicine, Kyoto, Japan;* [3]*Louis Pasteur Center for Medical Research, Kyoto, Japan;* [4]*Department of Cardiovascular Surgery, Saitama Medical Center, Kawagoe, Saitama, Japan and* [5]*Department of Inflammation and Immunology, Kyoto Prefectural University of Medicine, Kyoto, Japan*

Catheter-mediated, percutaneous, transluminal delivery of naked plasmid DNA (pDNA) into myocardium may offer a valuable strategy to heart diseases. Here, we examined whether clinically available transthoracic direct current (DC) shock improves intracoronary naked DNA transfection into myocardium. Plasmid vector encoding the GL3 luciferase was infused retrogradely into the coronary veins of beagle dogs, whereas another pDNA solution was infused into the left coronary artery. During and after these procedures, the coronary venous sinus was occluded by balloon, and transthoracic DC shock of 200 J was applied immediately after the infusions. Without DC shock, no remarkable increase in luciferase activity was demonstrated in any part of the left ventricular myocardium. In the presence of DC pulsation, significant luciferase expression was detected in the regions that were supplied by left anterior descending coronary artery (LAD), whereas the gene expression in the right coronary artery (RCA) regions was much less drastic. X-gal (5-bromo-4-chloro-3-indolyl-β-D-galactoside) staining of cardiac cross-sections also revealed regional expression of β-galactosidase. Immunohistochemical examinations of heart cryosections revealed that cardiomyocytes in LAD regions successfully expressed transgene product. The present system may enable a new strategy for myocardial gene therapy, without any special device or technique other than cardiac catheterization and DC cardioversion that are generally performed in ordinary hospitals.

Gene Therapy (2006) **13,** 906–916. doi:10.1038/sj.gt.3302742; published online 2 March 2006

Keywords: *coronary infusion; naked plasmid DNA; nonviral gene delivery; myocardium; transthoracic direct current shock*

Introduction

As a research tool to investigate the pathophysiological and molecular mechanisms of cardiovascular disorders, and as an essential means of gene therapy for heart diseases, a gene transfer technique that is highly efficient, repeatable and widely applicable without myocardial toxicity is desired. Currently, *in vivo* gene transfer into myocardium is performed by direct intracardiomuscular injection[1–8] or transcoronary infusion[4,9–12] of viral vectors[1–4,9–12] or nonviral vectors.[5–8] The usefulness of viral vectors, including retrovirus vectors, adenovirus vectors and adeno-associated virus (AAV) vectors, has been accepted owing to their high transduction efficiency. However, viral vector-based transduction may cause severe side effects, for example, possible insertional mutagenesis induced by retrovirus vectors and inflammatory responses induced by adenovirus vectors. Recent improvements in AAV vectors enabled efficient intracardiac genetic transduction without significant toxicity,[13–15] but AAV vectors accommodate only relatively small DNA inserts, and infection *in vivo* with an AAV vector may induce antibody, which limits the effectiveness of repetitive administrations.

In contrast, naked DNA methods are advantageous over viral vectors, in terms of low toxicity, low immunogenicity and absence of restriction on the insert size. Another important advantage of naked DNA is their large-scale, affordable manufacture. However, critical shortage of nonviral gene delivery systems is that the transfection efficiency and the expression level are relatively insufficient.[16,17] To overcome these problems, physical methods, including the gene gun procedure,[18] have been investigated. Ultrasonic wave-mediated transduction of the plasmid DNA (pDNA)-microbubble conjugates has also been devised.[19–21] These physical nonviral procedures, as well as synthetic nonviral vectors such as cationic lipids[22–24] and cationic polymers,[25,26] remain impractical for treating patients with heart diseases, mainly because of their lack of effectiveness.

Correspondence: Dr O Mazda, Department of Microbiology, Kyoto Prefectural University of Medicine, Kamikyo, Kyoto 602-8566, Japan.
E-mail: mazda@koto.kpu-m.ac.jp
[6]These authors contributed equally to this work.
Received 15 August 2005; revised 12 January 2006; accepted 15 January 2006; published online 2 March 2006

Another promising method to increase naked DNA transduction efficiency is electroporation. In this method, application of an electric field forms pores in the lipid membrane, allowing influx of extracellular substances such as nucleic acids into the cell.[27] Electroporation has the following advantages: (1) genes may be introduced into any tissues or cells, (2) the procedure is easy and very rapid, requiring application of the electric field for only a few seconds, (3) the amount or size of DNA used is not stringently restricted, compared with the limitation in other gene delivery procedures, (4) introduction of genes can be limited to the region charged with an electric field, (5) repeated DNA administration is possible because of low immunogenicity and (6) the procedure requires no special skill and is inexpensive. Therefore, electroporation has been applied to not only cultured cells *in vitro* but also to organs/tissues *in vivo*,[28,29] including skeletal muscle,[30,31] liver,[32,33] skin,[34–36] cornea,[37] blood vessels[38] and synovium of joints.[39] Furthermore, tumors such as malignant melanoma,[40–43] glioma[44] and hepatocellular carcinoma[45] are good targets of electroporation.

As far as we know, however, there has been no report of electroporation applied to heart *in vivo*. The major reasons may be the necessity of invasive treatment, such as thoracotomy to directly attach the electrodes to the heart, and the possibility of side effects, such as arrhythmia. Indeed, today's electroporation instruments cannot easily be applied to the heart because of their risk to the patients. Meanwhile, transthoracic direct current (DC) shock has been widely applied to the heart, safely and effectively, in clinical practice for antiarrhythmic purposes for more than 50 years.[46] If these instruments are applicable to electrical gene transduction, then genetic treatment of the heart may be performed safely, effectively and at a low cost. In this study, to investigate the efficacy of gene transduction into cardiac muscle, transthoracic DC shock was administered after an intravascular injection of pDNA via a coronary catheter in canines.

Results

Transthoracic direct current shock enhances genetic transfer in vivo *into myocardium*

We first attempted intracoronary delivery of naked pDNA as a means for *in vivo* gene transfer into myocardium. pGEG.GL3, at a dose of 15 000 μg/15 ml, was divided into two aliquots and subjected to two consecutive retrograde intravenous bolus infusions into the coronary sinus. The heart was excised 1.5 days after infusion. The left ventricle (LV) was sectioned into 22 blocks as shown in Figure 1a, and the luciferase expression in each block was assayed. Very low luciferase expression was observed in all the regions tested (data not shown). Next, to achieve more persistent contact of pDNA with the cardiac tissue under high pressure, retrograde intravenous infusion of pGEG.GL3, at a total of 7000 μg, was performed after occlusion of the

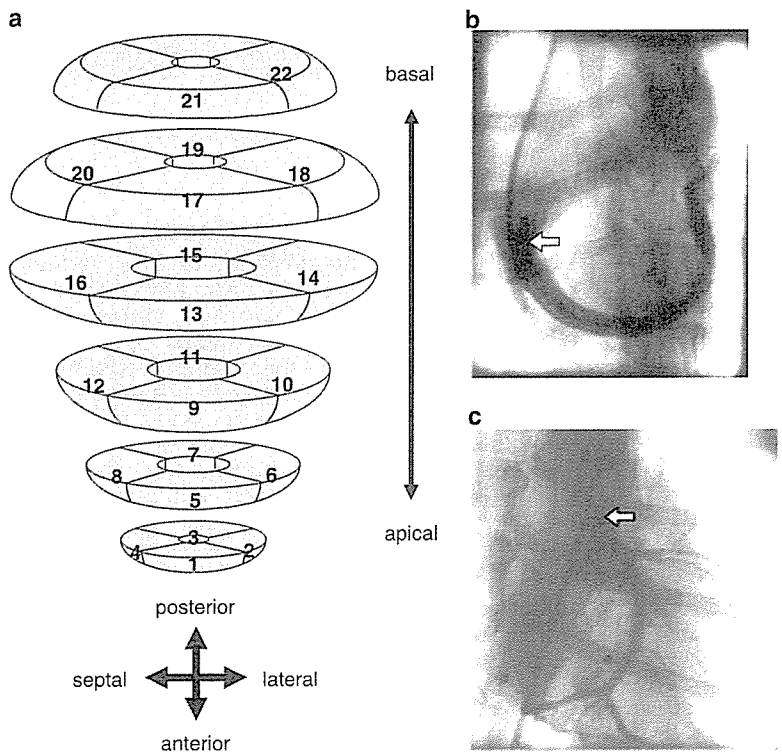

Figure 1 Experimental procedures. (**a**) Schematic illustration of heart sections. The left ventricle (LV) of the excised heart was sectioned into the 22 blocks as shown. (**b** and **c**) Intraoperative chest radiogram demonstrating the percutaneous catheter-mediated infusions. A fluid-filled balloon catheter was placed in the coronary venous sinus (**b**). A coronary catheter was placed in the ostium of the left coronary artery (**c**). The arrows in (**b**) and (**c**) indicate the catheter tips.

coronary sinus with a balloon, whereas antegrade infusion into the left coronary artery was concomitantly performed (protocol A; Figure 1b and c). Again, the luciferase gene expression after 1.5 days was very low, even at the heart blocks corresponding to the LAD regions that are supplied by the left anterior descending coronary artery (LAD; Figure 2a).

Then, we tried concomitant transthoracic DC shock with infusions into the coronary vein and artery, assuming that pulsed electric fields may promote delivery of pDNA into cardiomyocytes. After balloon occlusion of the coronary sinus, 200-J pulses were applied twice simultaneously with retrograde and antegrade intracoronary administrations of pGEG.GL3 at a total dose of 7000 μg (protocol B). After 1.5 days, significant luciferase expression was seen in many blocks (Figure 2b). To statistically analyze the data, we calculated the luciferase activities in six parts (proximal, middle and distal areas of LAD and right coronary artery (RCA) regions), based on the anatomical distribution of the coronary arteries in each dog.

The statistical data are shown in Figure 3a. The luciferase expression was markedly increased in the distal (32 000$\pm$5200 pg/mg protein), middle (29 000$\pm$

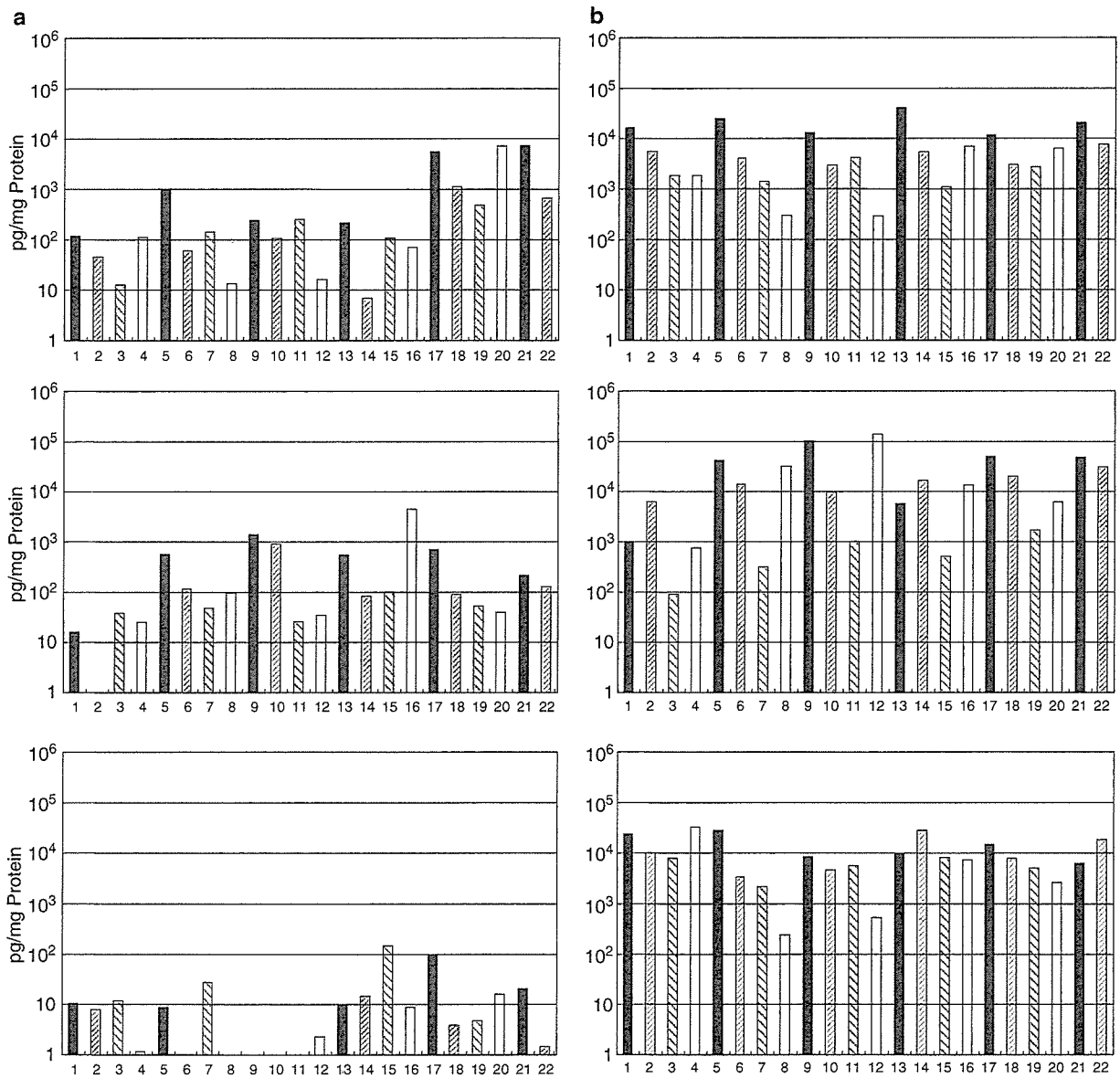

Figure 2 Luciferase expression 1.5 days after plasmid infusion. Hearts were transfected with pGEG.GL3 by protocol A (left panels, **a**) or protocol B (right panels, **b**) as described in Materials and methods ($n=3$ for each group. Each panel represents data from a single dog.) One and a half days later, the hearts were excised and sectioned into 22 blocks (see Figure 1b). Luciferase activity and protein content in the lysate of each block were measured. Numbers on the horizontal axes represent the LV blocks Nos (see Figure 1a). Closed, dark hatched, light hatched and open bars represent anterior blocks (nos. 1, 5, 9, 13, 17 and 21), lateral blocks (nos. 2, 6, 10, 14, 18 and 22), posterior blocks (nos. 3, 7, 11, 15 and 19) and septal blocks (nos. 4, 8, 12, 16 and 20), respectively (see Figure 1a).

7000 pg/mg protein) and proximal (29 000±9400 pg/mg protein) LAD regions, showing that concomitant DC shock drastically promoted gene transfer into heart muscle. The results were in sharp contrast to those obtained by pDNA infusion without DC pulsation (*P*-values between protocol A and B groups = 0.004, 0.02 and 0.05, for the distal, middle and proximal LAD regions, respectively; Figure 3a).

As a control experiment for protocol B, pGEG.EGFP lacking the luciferase gene was infused at a total dose of 7000 μg and DC pulsation was applied. On day 1.5, luciferase expression was not significantly detected in any regions tested (data not shown).

Localization of gene expression

In the canine hearts subjected to protocol B, high expression of luciferase was observed in LAD regions (Figure 3a). In sharp contrast, the expression was generally low in the blocks corresponding to the regions that were supplied by the RCA (Figure 1a). To statistically demonstrate the localization of the gene expression, the luciferase levels in the LAD and RCA regions were compared. It was clearly shown that the transduction rate was significantly higher in both distal (32 000±5200 vs 1300±540 pg/mg protein, $P = 0.005$) and middle (29 000±7000 vs 3200±2500 pg/mg protein, $P = 0.03$) LAD regions (Figure 3b). The proximal LAD regions showed a tendency to express higher luciferase levels than the proximal RCA regions, although statistically significant difference was not demonstrated between these regions (30 000±10 000 vs 3200±1000 pg/mg protein, $P = 0.06$; Figure 3b).

To investigate where in the LAD regions the gene was introduced, the anterior wall was excised from the canines 1.5 days after being subjected to protocol B, and divided into the endocardial, middle and epicardial layers. The luciferase gene was strongly expressed predominantly in the epicardial layer (23 000±8400 pg/mg protein), but much less expressed in the middle (7700±2200 pg/mg protein) and endocardial (3200±570 pg/mg protein) layers (Figure 3c).

To histologically identify the genetically modified regions, the heart was transfected with a β-galactosidase (β-gal)-containing plasmid construct, pGEG.β, by protocol B and subjected to X-gal (5-bromo-4-chloro-3-indolyl-β-D-galactoside) staining. As shown in Figure 4a, the expression of β-gal was detected mainly in the anterior septum, which was consistent with the results of the luciferase assay (Figure 2b). In another experiment in which pGEG.GL3 was transfected into a dog by protocol B, cross-sections of the heart were not significantly stained with X-gal (Figure 4b). The results clearly indicate that the positive X-gal staining of the β-gal gene-transfected heart (Figure 4a) was not owing to nonspecific staining or cell injury.

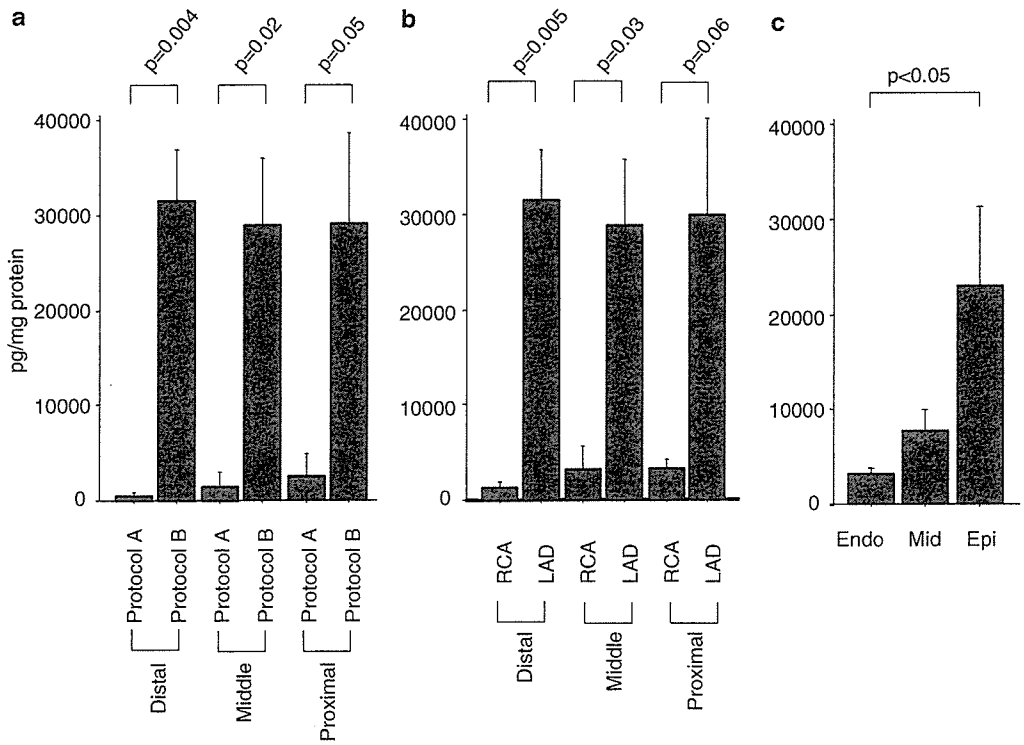

Figure 3 Comparison among protocols and localization of marker gene expression. (a) Hearts were transfected with pGEG.GL3 by protocols A and B as indicated. The average±s.d. of luciferase activities (day 1.5) were calculated for left ventricle (LV) blocks at distal, middle and proximal left anterior descending coronary artery (LAD) regions ($n = 3$ for each group). (b) Hearts were transfected with pGEG.GL3 by protocol B. The average±s.d. of luciferase activities (day 1.5) were calculated for LV blocks at distal, middle and proximal areas of LAD and right coronary artery (RCA) regions ($n = 3$ for each group). (c) One and a half days after transfection with pGEG.GL3 by protocol B, LAD regions of left ventricle (LV) was divided into three layers, that is, endocardial, middle and epicardial layers. The average±s.d. of luciferase activity was calculated.

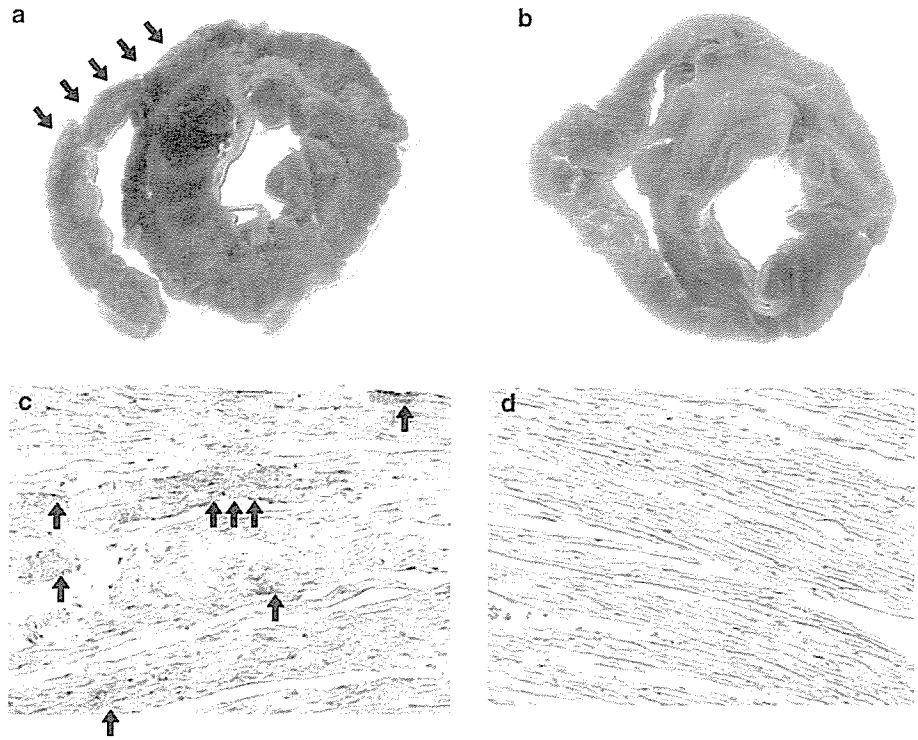

Figure 4 Localization of marker gene expression. (**a** and **b**) Shown are representative X-gal (5-bromo-4-chloro-3-indolyl-β-D-galactoside)-stained cross-sections of myocardium obtained 5 days after transfection with pGEG.β (**a**) or 1.5 days after pGEG.GL3 transfection (**b**) by protocol B. Arrows indicate cardiac muscle staining with X-gal (green). (**c** and **d**) Shown are representative immunohistochemical staining of myocardial cryosections obtained 1.5 days after transfection with pGEG.EGFP (**c**) or pGEG.GL3 (**d**) by protocol B (original magnification, $\times$200). Arrows indicate cardiomyocytes staining with anti-green fluorescent protein (GFP) antibody (brown).

To investigate which cell type in the heart was transfected, pGEG.EGFP was transduced into the heart by protocol B, and cryosections of the heart were subjected to immunohistochemical staining with anti-enhanced green fluorescent protein (EGFP) antibody. Figure 4c shows a representative microscopic image. It was revealed that 20–25% of cardiomyocytes successfully expressed the transgene product. The electrotransfection with a control plasmid did not result in EGFP expression at a detectable level (Figure 4d).

The expression level of Luc remained high on day 5 after transfection (Figure 5c), whereas on day 12, the Luc activity was very low, if any (data not shown). The findings suggest that the transgene expression induced by electrotransfection does not persist for more than 12 days.

Influence of vascular malformation on gene transfer

Persistent left superior vena cava (LSVC) was observed in one dog (Figure 5d). When the coronary sinus was occluded with a balloon, and retrograde intravenous infusion of contrast medium was performed, the contrast medium was not pooled in the vein, and was washed out through the angiectopia. Gene transduction using protocol B was performed in this animal, and localization of the luciferase expression was investigated on day 5. Compared with the normal dog (Figure 5a), the level of expression was similar in the apex of the heart, but very low in the basal regions (Figure 5b), suggesting that anomaly of coronary vasculature affected the genetic transfection. Regarding localization, the expression was predominant in the anterior wall, as in the normal dogs.

Side effect of cardiac catheterization and gene delivery

Intraoperative balloon occlusion of the coronary sinus decreased blood pressure and elevated the ST segment in the electrocardiogram (a representative electrocardiogram is shown in Figure 6a). These findings may have reflected the ischemic condition in the heart. When the coronary sinus was occluded for 40 s after retrograde intravenous infusion or for 150 s without intravenous infusion, a mild elevation of the ST segment was observed during the occlusion, but this electrocardiographic (ECG) change was rapidly recovered after balloon deflation.

Transient ventricular arrhythmia occurred immediately after DC shock in some animals treated with protocol B, but sinus rhythm was rapidly resumed after intravenous administration of 20 mg lidocaine, and no problematic complication occurred.

In an animal that received a retrograde intravenous infusion, occlusion was maintained for a longer period to assess possible side effects of the procedure. On electrocardiography, the degree of ST elevation was drastically increased after about 40 s of occlusion, with mild prolongation of the QRS interval. When occlusion was further continued, severe hypotension and ventricular fibrillation occurred. The balloon was deflated at this point, but the animal died despite an attempt of defibrillation by lidocaine administration and DC shock.

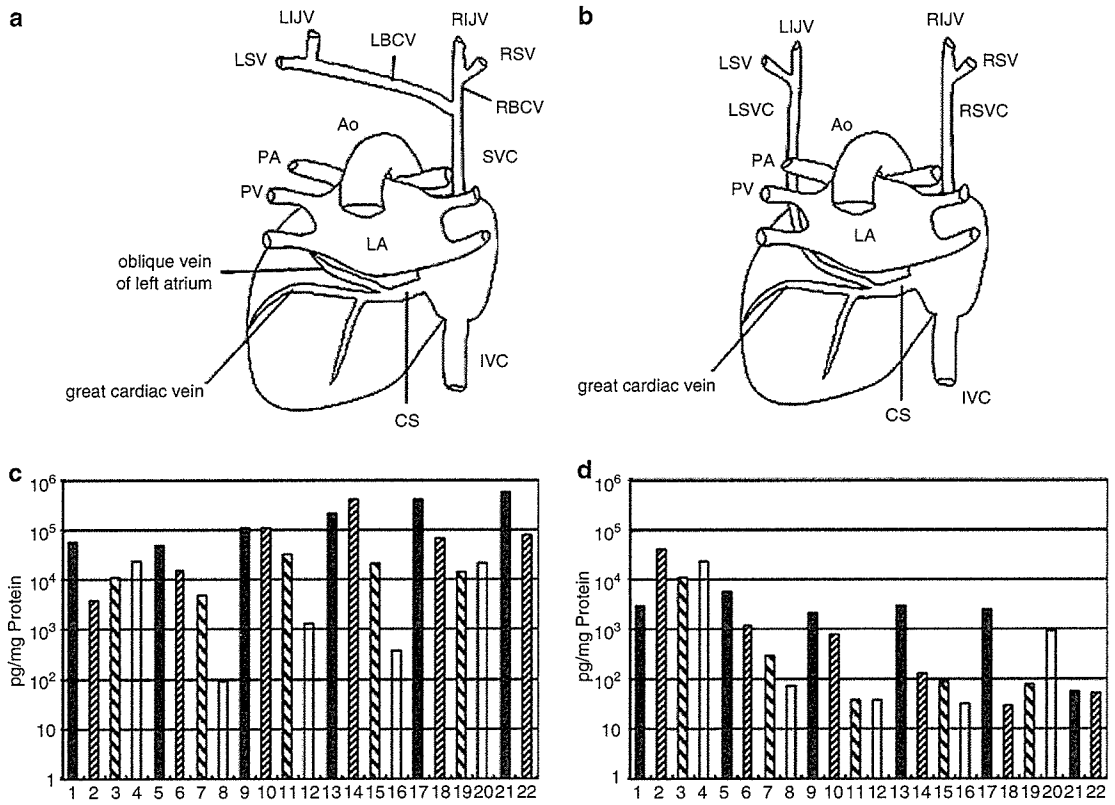

Figure 5 Vascular malformation influenced direct current (DC)-mediated transcoronary plasmid DNA (pDNA) transfection. (**a** and **b**) Schematic illustrations of the heart and great vessel systems (back views). A dog had the persistent left superior vena cava (PLSVC; shaded line in **b**), which is lacking in normal dogs (**a**). Ao, aorta; LA, left atrium; PV, pulmonary vein; IVC, inferior vena cava; SVC, superior vena cava; BCV, brachiocephalic vein; SV, subclavian vein; IJV, internal jugular vein. (**c** and **d**) Normal (**c**) and PLSVC (**b**) hearts were transfected with pGEG.GL3 by protocol B, and 5 days later the hearts were sectioned into 22 blocks. Luciferase activity and protein content were measured as in Figure 2. Numbers on the horizontal axes represent the left ventricle (LV) blocks Nos (see Figure 1a). Closed, dark hatched, light hatched and open bars represent anterior blocks (nos. 1, 5, 9, 13, 17 and 21), lateral blocks (nos. 2, 6, 10, 14, 18 and 22), posterior blocks (nos. 3, 7, 11, 15 and 19) and septal blocks (nos. 4, 8, 12, 16 and 20), respectively; see Figure 1a).

In the dogs treated with concomitant retrograde intravenous and antegrade intracoronary delivery with transthoracic DC shock (protocol B), echocardiography was performed before and 5 days after the gene transduction to investigate changes in the cardiac function. The LV remained normokinetic before and after gene transduction, without any evidence of localized abnormal wall movement (Figure 6b). No significant changes were observed in the ventricular wall thickness, chamber size or fractional shortening (FS), showing that the treatment did not reduce the contractility of the LV (Table 1).

We also performed biochemical analyses of dog sera before and after transfection by protocols A and B. Although MB fraction of creatinine phosphokinase (CPK-MB) slightly elevated after the transfection, the level decreased to normal range by day 1.5 (Table 2). Any significant change was not seen in cardiac troponin T (cTnT) and C-reactive protein (CRP) levels before, immediately after and 1.5 days after gene transfer (Table 2). The histopathological examination of heart sections did not show any significant sign of inflammation or cell injury on days 1.5 (Figure 4c) and 5 (data not shown). Gross morphological observation of cardiac cross-sections also failed to reveal any evidence of inflammation 12 days after electrotransfection (data not shown).

Discussion

In this study, we succeeded in percutaneous transluminal gene transfer into myocardium. In 16 dogs, the coronary sinus was occluded with a balloon to transiently pool the plasmid in the coronary vessels. Ten of the dogs received transthoracic DC shock, aiming at electric gene delivery. Coronary gene administration with concomitant transthoracic DC shock allowed efficient gene transduction.

Percutaneous catheter-mediated intracoronary delivery appears to be the most clinically relevant method, because of the capabilities of obtaining gene transduction in a specific region by choosing a coronary artery or vein that perfuses the target region, and because transduction in the target region is relatively homogeneous, compared with the direct intracardiomuscular injection method. Because of these advantages, transluminal procedures may be very useful when transduction into a wide area is necessary, such as in gene therapy for cardiomyopathy and cardiac failure.

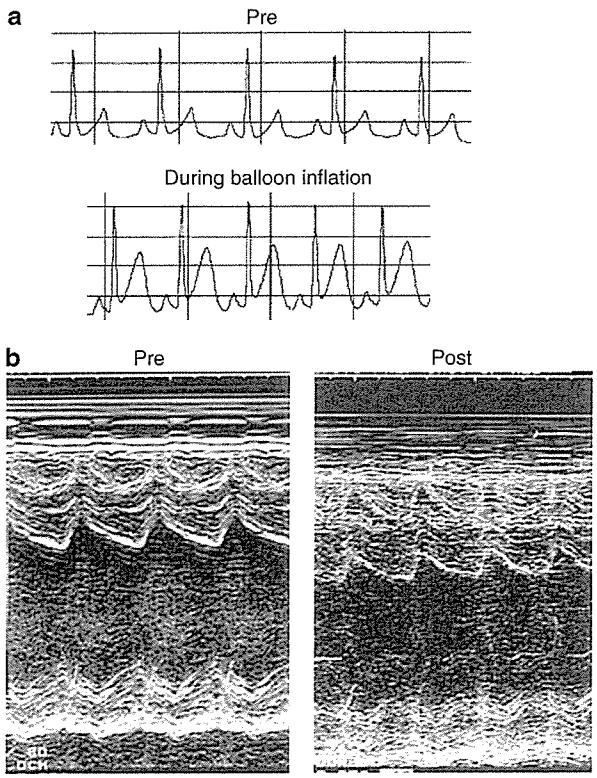

Figure 6 Electrocardiographic and echocardiographic monitoring of cardiac function. (**a**) Representative electrocardiographic patterns before (upper panel) and 40 s after (lower panel) the balloon occlusion of coronary venous sinus. (**b**) Representative echocardiographic images before (left panel) and 5 days after (right panel) the pGEG.GL transfection by protocol B.

Table 1 Echocardiographic assessment of cardiac function

n=3	*Before*	*5 Days after the gene transduction*	*P-value*
Dd (mm)	32±1.4	33±1.0	NS
Ds (mm)	25±1.2	25±0.9	NS
FS (%)	24±1.2	25±2.5	NS
EF (%)	50±2.0	51±3.7	NS
PW (mm)	5.6±0.0	5.6±0.2	NS

Dd: end-diastolic dimension; Ds: end-systolic dimension; EF: ejection fraction; FS: fractional shortening; NS: not significant; PW: posterior LV wall.
For three dogs, hearts were transfected with pGEG.GL3 by the protocol B, and echocardiographic examination was performed before and 5 days after the gene transduction.

Some previous studies also reported *in vivo* genetic transduction into the heart of large animals. Boekstegers *et al.*[11] transduced an adenovirus vector carrying luciferase gene into the heart of German farm pig, by means of selective pressure-regulated retroinfusion through the coronary veins with coronary artery occlusion, resulting in luciferase expression in endocardium of LAD at approximately 74 000 relative luciferase units (RLU)/mg protein/30 s. March *et al.*[47] injected an adenovirus vector directly into the intrapericardial space of the mongrel dogs, showing that Luc expression reached 50 000 and <1000 RLU/mg protein/10 s in LV epicardium and endocardium, respectively. von Harsdorf *et al.*[48] performed direct naked pDNA injection into the epicardium in mongrel dogs, and Luc expressed at approximately 2200 RLU/mg protein/20 s. Our electrotransfection method may be inferior to the adenovirus-mediated transduction, but superior to naked pDNA injection, in terms of the Luc expression in myocardium of large animals

Table 2 Examination of biochemical parameters

Dog (no.)	*Pre*	*Post*	*Day 1.5*
CPK-MB (ng/ml)			
1	5.3	6.2	3.0
2	7.7	11.9	2.0
3	3.1	6.1	3.4
cTnT (ng/ml)			
1	0.02	0.02	0.02
2	0.02	0.02	0.02
3	0.02	0.06	0.09
CRP (mg/dl)			
1	0.1	0.1	0.5
2	0.1	0.1	0.3
3	0.5	0.4	0.5

CPK: creatinine phosphokinase; CRP: C-reactive protein; cTnT: cardiac troponin T.
Hearts were transfected with pGEG.GL3 by the protocol A (dog no. 1) or B (dogs no. 2 and no. 3) and serum examination was performed before (pre), immediately after (post) and 1.5 days after (day 1.5) the gene transduction.

In mice, a rapid tail vein injection of naked pDNA induces a tremendously high-level expression of exogenous genes in the liver,[49–52] whereas the procedure also results in significant gene delivery into the heart, albeit at a considerably lower rate.[50,52] The skeletal muscle is also effectively transfected by intraarterial injection of pDNA in non-human primate.[53] In the present study, we obtained only low-level transgene expression in cardiomyocytes after intracoronary infusion of pDNA without electric pulsation (Figure 2a and data not shown), although the experiments were performed at a condition that may be suitable for naked DNA infusion (the dose of pDNA was 350 μg/kg body weight, and assay was performed on day 1.5). This may have been related to species differences in sizes of the organ and vascular lumen, coronary vasculature, flow volume and velocity of the coronary circulation, as well as biochemical characteristics of cardiomyocytes. Alternatively, the failure of intravascular pDNA transfection into cardiac muscle may be ascribed to insufficient pressure owing to the devices that were employed in this large animal model.

It is interesting to note that DC shock generates exponentially decaying wave pulses rather than square wave pulses. The efficiencies of electric gene transfer are highly affected by the electric field strength and pulse shapes. It is generally believed that square wave pulses are superior to exponentially decaying pulses, because the pulse duration and amplitude can be controlled independently,[54] and electroporation devices are designed accordingly. Square wave pulses of low field strength have been popularly employed in electroporation *in vivo*, whereas exponentially decaying wave pulses

have been used rarely.[54,55] However, Andreason *et al.*[56] previously reported that an exponentially decaying wave pulse was suitable for electrotransfection *in vitro*, as it provided both the initial high voltage required for poration and the following low voltage 'tail' for electophoretical transfer of DNA molecules into the cell. The present study suggests that *in vivo* electroporation may also be achieved using not only square wave pulses but also exponentially decaying pulses, whereas the feasibility of another waveform was also presented recently.[57]

It is conceivable that, to increase the transduction efficiency, the operation procedure should be designed in such a manner that the coronary vessel be in contacted with a high density of plasmid for a long time during the DC shock. The DC shock-dependent transduction was more effective when both intravenous infusion and intraarterial infusion were used together (protocol B), compared with when either of the two routes was used alone (data not shown).

The susceptibility of the cardiac muscle to ischemia poses a major challenge. Actually, in the animal in which the coronary sinus was occluded with a balloon for a prolonged period following retrograde intravenous infusion, severe hypotension and ventricular fibrillation was fatal (see 'Results'). Electrocardiographic monitoring should therefore be performed to detect ischemic change and arrhythmia, which may be induced by coronary balloon occlusion during the transfection procedure.

A balloon with a smaller diameter was applied to one dog during protocol B. No significant ST change was observed on ECG, suggesting that ischemia did not occur owing to insufficient occlusion. Interestingly, the transfection rate was very low in the heart of this dog (data not shown), suggesting the necessity of occlusion of the coronary sinus. As for the practicality of the present system for gene therapy of cardiac diseases, ECG changes should be confirmed on a case-by-case basis to demonstrate sufficient occlusion of the coronary vein, in order that efficient gene transduction can be achieved in the patient (Figure 6a).

Another dog subjected to protocol B had congenital anomaly in cardiovascular morphogenesis, that is, the persistent left superior vena cava, as demonstrated by cardioangiography (Figure 5b). Owing to a failure of regression of left anterior and common cardinal veins as well as left sinus horn, LSVC starts at the junction of left subclavian vein and left internal jugular, passes lateral to aortic arch and finally receives great cardiac vein to drain into coronary sinus (Figure 5d). When the coronary sinus was occluded with a balloon and plasmid solution was infused into the coronary veins, the plasmid solution was washed out through the LSVC rather than pooled in the coronary vein. As the results, gene transduction was very low, except for in the apical region (Figure 5b). This finding suggests that variation of the coronary vasculature among individuals affects the success rate of transfection into cardiac muscular regions. Therefore, the coronary vasculature of each patient should be checked by angiography before gene therapy.

Finally, it should be emphasized that the procedure does not require any specific device other than regular instruments used in ordinary hospitals, nor does it require of the cardiologists to have additional skills. This method may be applicable to gene therapy not only as a local treatment such as promotion of neovascularization in ischemic heart diseases but also for cases with wide lesions requiring repeated therapy such as in cardiac failure.

Materials and methods

Animals

Eight-month-old female beagle dogs weighing 9.1–10.4 kg were purchased from Oriental BioService (Kyoto, Japan). They received humane care in accordance with the institutional guidelines of Kyoto Prefectural University of Medicine.

Plasmid vectors

The plasmid vectors have been described previously. Briefly, pGEG.GL3,[52] pGEG.β[58] and pGEG.EGFP[39] carry the GL3 firefly luciferase (derived from pGL3-Basic Vector; Promega, Madison, WI, USA), *Escherichia coli* β-gal and the EGFP genes, respectively, under the control of the CAG promoter, whereas both plasmids also contain Epstein–Barr virus (EBV) nuclear antigen 1 gene, EBV oriP sequence and the ampicillin-resistant gene.[17] The plasmids were purified using EndoFree plasmid purification system (Qiagen, Hilden, Germany).

Cardiac catheterization and gene delivery

The dogs were sedated with an intramuscular administration of 100 mg ketamine, 30 mg xylazine and 0.5 mg atropine, and ventilated mechanically. Anesthesia was maintained by intravenous administrations of 50 mg ketamine every 30 min.

A 5F catheter introducer sheath (Medikit, Tokyo, Japan) was placed in the right femoral artery, and a 7F sheath was placed in the right external jugular vein. After an intravenous injection of 5000 U heparin and 20 mg lidocaine, a 5.0×40 mm fluid-filled balloon catheter (Cordis, Miami, FL, USA) and a 4F coronary catheter (Medikit) were placed under fluoroscopic guidance in the coronary venous sinus and the left coronary artery, respectively.

Plasmid vectors were delivered under the following conditions. Protocol A: pGEG.GL3 at a dose of 3500 μg was diluted in 10 ml of saline and infused as a 5-s bolus retrogradely into the coronary vein through the lumen of the 'over the wire' balloon catheter, whereas another pGEG.GL3 solution (1750 μg/5 ml saline) was infused simultaneously as a 5-s bolus into the left coronary artery. During and after these procedures, the coronary venous sinus was occluded for 40 s by balloon inflation. Immediately after the manipulation, pGEG.GL3 solution (1750 μg/5 ml saline) was infused as a 5-s bolus into the coronary artery with occlusion of coronary venous sinus for 150 s. Protocol B: As protocol A except transthoracic DC shock of 200 J was applied immediately after the infusions into the coronary artery and vein. A commonly available clinical use instrument was used for the DC shock (TEC 7621, Nihon Kohden, Tokyo, Japan). In some experiments, pGEG.β or pGEG.EGFP was infused instead of pGEG.GL3.

After the procedures, all catheters and introducer sheaths were removed, the vessels were ligated and the wound surgically closed (day 0).

Luciferase assay

The dogs were killed and the heart was perfused with heparinized saline solution (1 U/ml) infused via the aortic root. The LV of the excised heart was sectioned into the 22 blocks as shown in Figure 1a. Because each dog shows slight anatomical variation in coronary circulation, location of LAD and RCA was precisely recorded for each dog, so that raw data for the 22 blocks were pooled to calculate luciferase activities in distal, middle and proximal areas in LAD and RCA regions in subsequent statistical analyses (see below). In an experiment, epicardial, middle and endocardial layers were separated from each block, whereas in other experiments, epicardial layer of each block was collected. These specimens were homogenized in 200 μl reporter lysis buffer (Promega) using a sonicator. The extract was centrifuged at 10 000 *g* for 5 min. Luciferase activity in the supernatant was measured using a Luciferase Assay Kit (Promega) as described previously.[52] Photoemission was measured during a 10-s period using a luminometer. Protein concentration in the supernatant was measured as described.[52]

Statistical analyses

For statistical comparisons between two groups (protocols A vs B, and LAD vs RCA regions), differences were analyzed by unpaired *t*-test. For statistical comparisons among three groups (epicardial, middle and endocardial layers), differences were tested by analysis of variance with Schffe's correction. A value of $P<0.05$ was considered to be statistically significant.

X-gal staining

The heart was excised and horizontally sectioned into 3-mm-thick slices (from apex to basis). The slices were washed in phosphate-buffered saline (PBS) and incubated in X-gal staining solution (0.05% (v/v) X-gal (Nacalai Tesque, Kyoto, Japan), 1 mM $MgCl_2$, 150 mM NaCl, 3 mM $K_4[Fe(CN)_6]$, 3 mM $K_3[Fe(CN)_6]$, 60 mM Na_2HPO_4, 40 mM NaH_2PO_4 and 0.1% Triton X-100) for 4 h at 37°C. The reaction was terminated by replacing the solution with 1 mM Na_2-EDTA/PBS.[59]

Immunohistochemistry

After perfusion with saline, the heart was excised, fixed with 4% paraformaldehyde and dehydrated in sucrose solution. The specimens were embedded in OCT compound and immediately frozen at −80°C. Serial sections 6 μm thick were sliced on a cryostat, and stained with anti-GFP immunoglobulin (Molecular Probes, Leiden, the Netherlands) followed by visualization with the ABC method (VECTASTAIN elite ABC kit; Vector Laboratories, Inc., Burlingame, CA, USA). Sections were stained with hematoxylin after the immunohistochemical staining.

Electrocardiographic and echocardiographic examinations

Echocardiograhic studies were performed under anesthesia with an intramuscular administration of 100 mg ketamine, 30 mg xylazine and 0.5 mg atropine. A two-dimensional parasternal short-axis view of the LV was obtained at the level of the papillary muscles using echocardiographic system equipped with a 2.5 MHz phased-array transducer (SONOLAYER SSH-160A; Toshiba, Tokyo, Japan). The LV end-diastolic dimension, LV end-systolic dimension, FS, ejection fraction, end-diastolic interventricular septum thickness and end-diastolic posterior LV wall thickness were measured.

Examination of biochemical parameters

Sera were obtained before, immediately after and 1.5 days after gene transfer. Biochemical parameters including the CPK-MB, cTnT and CRP were measured by ADVIA Centaur immunoassay analyzer (Bayer Medical, Tokyo, Japan), ECLusys 2010 immunoassay analyzer (Roche Diagnostics, Tokyo, Japan) and Clinical Analyzer 7700 multiple automatic analyzer (Hitachi High-Technologies, Tokyo, Japan), respectively.

Acknowledgements

We thank Drs Yoshiki Itokawa and Hiroshi Nakano (Departments of Surgery and Otorhinolaryngology, Kyoto Prefectural University of Medicine, respectively) for assisting in the animal experiments.

References

1 Guzman RJ, Lemarchand P, Crystal RG, Epstein SE, Finkel T. Efficient gene transfer into myocardium by direct injection of adenovirus vectors. *Circ Res* 1993; **73**: 1202–1207.
2 French BA, Mazur W, Geske RS, Bolli R. Direct *in vivo* gene transfer into porcine myocardium using replication-deficient adenoviral vectors. *Circulation* 1994; **90**: 2414–2424.
3 Magovern CJ, Mack CA, Zhang J, Hahn RT, Ko W, Isom OW *et al*. Direct *in vivo* gene transfer to canine myocardium using a replication-deficient adenovirus vector. *Ann Thorac Surg* 1996; **62**: 425–434.
4 Svensson EC, Marshall DJ, Woodard K, Lin H, Jiang F, Chu L *et al*. Efficient and stable transduction of cardiomyocytes after intramyocardial injection or intracoronary perfusion with recombinant adeno-associated virus vectors. *Circulation* 1999; **99**: 201–205.
5 Lin H, Parmacek MS, Morle G, Bolling S, Leiden JM. Expression of recombinant genes in myocardium *in vivo* after direct injection of DNA. *Circulation* 1990; **82**: 2217–2221.
6 Acsadi G, Jiao SS, Jani A, Duke D, Williams P, Chong W *et al*. Direct gene transfer and expression into rat heart *in vivo*. *New Biol* 1991; **3**: 71–81.
7 Li K, Welikson RE, Vikstrom KL, Leinwand LA. Direct gene transfer into the mouse heart. *J Mol Cell Cardiol* 1997; **29**: 1499–1504.
8 Tomiyasu K, Oda Y, Nomura M, Satoh E, Fushiki S, Imanishi J *et al*. Direct intra-cardiomuscular transfer of beta2-adrenergic receptor gene augments cardiac output in cardiomyopathic hamsters. *Gene Therapy* 2000; **7**: 2087–2093.
9 Barr E, Carroll J, Kalynych AM, Tripathy SK, Kozarsky K, Wilson JM *et al*. Efficient catheter-mediated gene transfer into the heart using replication-defective adenovirus. *Gene Therapy* 1994; **1**: 51–58.
10 French BA, Mazur W, Ali NM, Geske RS, Finnigan JP, Rodgers GP *et al*. Percutaneous transluminal *in vivo* gene transfer by recombinant adenovirus in normal porcine coronary arteries, atherosclerotic arteries, and two models of coronary restenosis. *Circulation* 1994; **90**: 2402–2413.
11 Boekstegers P, von Degenfeld G, Giehrl W, Heinrich D, Hullin R, Kupatt C *et al*. Myocardial gene transfer by selective pressure-

regulated retroinfusion of coronary veins. *Gene Therapy* 2000; **7**: 232–240.
12 Logeart D, Hatem SN, Heimburger M, Le Roux A, Michel JB, Mercadier JJ. How to optimize *in vivo* gene transfer to cardiac myocytes: mechanical or pharmacological procedures? *Hum Gene Ther* 2001; **12**: 1601–1610.
13 Hoshijima M, Ikeda Y, Iwanaga Y, Minamisawa S, Date MO, Gu Y *et al.* Chronic suppression of heart-failure progression by a pseudophosphorylated mutant of phospholamban via *in vivo* cardiac rAAVgene delivery. *Nat Med* 2002; **8**: 864–871.
14 Agrawal RS, Muangman S, Layne MD, Melo L, Perrella MA, Lee RT *et al.* Pre-emptive gene therapy using recombinant adeno-associated virus delivery of extracellular superoxide dismutase protects heart against ischemic reperfusion injury, improves ventricular function and prolongs survival. *Gene Therapy* 2004; **11**: 962–969.
15 Su H, Joho S, Huang Y, Barcena A, Arakawa-Hoyt J, Grossman W *et al.* Adeno-associated viral vector delivers cardiac-specific and hypoxia-inducible VEGF expression in ischemic mouse heart. *Proc Natl Acad Sci* 2004; **101**: 16280–16285.
16 Niidome T, Huang L. Gene therapy progress and prospects: nonviral vectors. *Gene Therapy* 2002; **9**: 1647–1652.
17 Mazda O. Improvement of nonviral gene therapy by Epstein–Barr virus (EBV)-based plasmid vectors. *Curr Gene Ther* 2002; **2**: 379–392.
18 Nishizaki K, Mazda O, Dohi Y, Kawata T, Mizuguchi K, Kitamura S *et al. In vivo* gene gun-mediated transduction into rat heart with Epstein–Barr virus-based episomal vectors. *Ann Thorac Surg* 2000; **70**: 1332–1337.
19 Shohet RV, Chen S, Zhou YT, Wang Z, Meidell RS, Unger RH *et al.* Echocardiographic destruction of albumin microbubbles directs gene delivery to the myocardium. *Circulation* 2000; **101**: 2554–2556.
20 Vannan M, McCreery T, Li P, Han Z, Unger E, Kuersten B *et al.* Ultrasound-mediated transfection of canine myocardium by intravenous administration of cationic microbubble-linked plasmid DNA. *J Am Soc Echocardiogr* 2002; **15**: 214–218.
21 Chen S, Shohet RV, Bekeredjian R, Frenkel P, Grayburn PA. Optimization of ultrasound parameters for cardiac gene delivery of adenoviral or plasmid deoxyribonucleic acid by ultrasound-targeted microbubble destruction. *J Am Coll Cardiol* 2003; **42**: 301–308.
22 Shi Y, Fard A, Vermani P, Zalewski A. Transgene expression in the coronary circulation: transcatheter gene delivery. *Gene Therapy* 1994; **1**: 408–414.
23 Affleck DG, Yu L, Bull DA, Bailey SH, Kim SW. Augmentation of myocardial transfection using TerplexDNA: a novel gene delivery system. *Gene Therapy* 2001; **8**: 349–353.
24 Wright MJ, Wightman LM, Lilley C, de Alwis M, Hart SL, Miller A *et al. In vivo* myocardial gene transfer: optimization, evaluation and direct comparison of gene transfer vectors. *Basic Res Cardiol* 2001; **96**: 227–236.
25 Qin L, Pahud DR, Ding Y, Bielinska AU, Kukowska-Latallo JF, Baker Jr JR *et al.* Efficient transfer of genes into murine cardiac grafts by Starburst polyamidoamine dendrimers. *Hum Gene Ther* 1998; **9**: 553–560.
26 Lee M, Rentz J, Han SO, Bull DA, Kim SW. Water-soluble lipopolymer as an efficient carrier for gene delivery to myocardium. *Gene Therapy* 2003; **10**: 585–593.
27 Mir LM, Banoun H, Paoletti C. Introduction of definite amounts of nonpermeant molecules into living cells after electropermeabilization: direct access to the cytosol. *Exp Cell Res* 1998; **175**: 15–25.
28 Andre F, Mir LM. DNA electrotransfer: its principles and an updated review of its therapeutic applications. *Gene Therpy* 2004; **11** (Suppl 1): S33–S42.
29 Heller L, Ugen K, Heller R. Electroporation for targeted gene transfer. *Expert Opin Drug Delivery* 2005; **2**: 255–268.
30 Mir LM, Bureau MF, Rangara R, Schwartz B, Scherman D. Long-term, high level *in vivo* gene expression after electric pulse-mediated gene transfer into skeletal muscle. *C R Acad Sci III* 1998; **321**: 893–899.
31 Aihara H, Miyazaki J. Gene transfer into muscle by electroporation *in vivo*. *Nat Biotechnol* 1998; **16**: 867–870.
32 Heller R, Jaroszeski M, Atkin A, Moradpour D, Gilbert R, Wands J *et al. In vivo* gene electroinjection and expression in rat liver. *FEBS Lett* 1996; **389**: 225–228.
33 Suzuki T, Shin BC, Fujikura K, Matsuzaki T, Takata K. Direct gene transfer into rat liver cells by *in vivo* electroporation. *FEBS Lett* 1998; **425**: 436–440.
34 Titomirov AV, Sukharev S, Kistanova E. *In vivo* electroporation and stable transformation of skin cells of newborn mice by plasmid DNA. *Biochim Biophys Acta* 1991; **1088**: 131–134.
35 Vanbever R, Preat V. *In vivo* efficacy and safety of skin electroporation. *Adv Drug Deliv Rev* 1999; **35**: 77–88.
36 Heller R, Schultz J, Lucas ML, Jaroszeski MJ, Heller LC, Gilbert RA *et al.* Intradermal delivery of interleukin-12 plasmid DNA by *in vivo* electroporation. *DNA Cell Biol* 2001; **20**: 21–26.
37 Oshima Y, Sakamoto T, Yamanaka I, Nishi T, Ishibashi T, Inomata H. Targeted gene transfer to corneal endothelium *in vivo* by electric pulse. *Gene Therapy* 1998; **5**: 1347–1354.
38 Schwachtgen JL, Ferreira V, Meyer D, Kerbiriou-Nabias D. Optimization of the transfection of human endothelial cells by electroporation. *Biotechniques* 1994; **17**: 882–887.
39 Ohashi S, Kubo T, Kishida T, Ikeda T, Takahashi K, Arai Y *et al.* Successful genetic transduction *in vivo* into synovium by means of electroporation. *Biochem Biophys Res Commun* 2002; **293**: 1530–1535.
40 Rols MP, Delteil C, Golzio M, Dumond P, Cros S, Teissie J. *In vivo* electrically mediated protein and gene transfer in murine melanoma. *Nat Biotechnol* 1998; **16**: 168–171.
41 Kishida T, Asada H, Satoh E, Tanaka S, Shinya M, Hirai H *et al. In vivo* electroporation-mediated transfer of interleukin-12 and interleukin-18 genes induces significant antitumor effects against melanoma in mice. *Gene Therapy* 2001; **8**: 1234–1240.
42 Lohr F, Lo DY, Zaharoff DA, Hu K, Zhang X, Li Y *et al.* Effective tumor therapy with plasmid-encoded cytokines combined with *in vivo* electroporation. *Cancer Res* 2001; **61**: 3281–3284.
43 Lucas ML, Heller L, Coppola D, Heller R. IL-12 plasmid delivery by *in vivo* electroporation for the successful treatment of established subcutaneous B16.F10 melanoma. *Mol Ther* 2002; **5**: 668–675.
44 Yoshizato K, Nishi T, Goto T, Dev SB, Takeshima H, Kino T *et al.* Gene delivery with optimized electroporation parameters shows potential for treatment of gliomas. *Int J Oncol* 2000; **16**: 899–905.
45 Heller L, Jaroszeski MJ, Coppola D, Pottinger C, Gilbert R, Heller R. Electrically mediated plasmid DNA delivery to hepatocellular carcinomas *in vivo*. *Gene Therapy* 2000; **7**: 826–829.
46 Beck CS, Pritchard WH, Feil SA. Ventricular fibrillation of long duration abolished by electric shock. *JAMA* 1947; **135**: 985–989.
47 March KL, Woody M, Mehdi K, Zipes DP, Brantly M, Trapnell BC. Efficient *in vivo* catheter-based pericardial gene transfer mediated by adenoviral vectors. *Clin Cardiol* 1999; **22**: I-123–I-129.
48 von Harsdorf R, Schott RJ, Shen YT, Vatner SF, Mahdavi V, Nadal-Ginard B. Gene injection into myocardium as a useful model for studying gene expression in the heart of large mammals. *Circ Res* 1993; **72**: 688–695.
49 Zhang G, Budker V, Wolff JA. High levels of foreign gene expression in hepatocytes after tail vein injections of naked plasmid DNA. *Hum Gene Ther* 1999; **10**: 1735–1737.
50 Liu F, Song Y, Liu D. Hydrodynamics-based transfection in animals by systemic administration of plasmid DNA. *Gene Therapy* 1999; **6**: 1258–1266.
51 Zhang G, Song YK, Liu D. Long-term expression of human alpha1-antitrypsin gene in mouse liver achieved by intravenous

administration of plasmid DNA using a hydrodynamics-based procedure. *Gene Therapy* 2000; **7**: 1344–1349.

52 Cui FD, Kishida T, Ohashi S, Asada H, Yasutomi K, Satoh E *et al.* Highly efficient gene transfer into murine liver achieved by intravenous administration of naked Epstei–Barr virus (EBV)-based plasmid vectors. *Gene Therapy* 2001; **8**: 1508–1513.

53 Zhang G, Budker V, Williams P, Subbotin V, Wolff JA. Efficient expression of naked DNA delivered intraarterially to limb muscles of nonhuman primates. *Hum Gene Ther* 2001; **12**: 427–438.

54 Gehl J. Electroporation: theory and methods, perspectives for drug delivery, gene therapy and research. *Acta Physiol Scand* 2003; **177**: 437–447.

55 Mir LM, Bureau MF, Gehl J, Rangara R, Rouy D, Caillaud JM *et al.* High-efficiency gene transfer into skeletal muscle mediated by electric pulses. *Proc Natl Acad Sci USA* 1999; **96**: 4262–4267.

56 Andreason GL, Evans GA. Optimization of electroporation for transfection of mammalian cell lines. *Anal Biochem* 1989; **180**: 269–275.

57 Lucas ML, Jaroszeski MJ, Gilbert R, Heller R. *In vivo* electroporation using an exponentially enhanced pulse: a new waveform. *DNA Cell Biol* 2001; **20**: 183–188.

58 Nakanishi H, Mazda O, Satoh E, Asada H, Morioka H, Kishida T *et al.* Nonviral genetic transfer of Fas ligand induced significant growth suppression and apoptotic tumor cell death in prostate cancer *in vivo*. *Gene Therapy* 2003; **10**: 434–442.

59 Tomiyasu K, Satoh E, Oda Y, Nishizaki K, Kondo M, Imanishi J *et al.* Gene transfer *in vitro* and *in vivo* with Epstein–Barr virus-based episomal vector results in markedly high transient expression in rodent cells. *Biochem Biophys Res Commun* 1998; **253**: 733–738.

Nox1 Is Involved in Angiotensin II–Mediated Hypertension

A Study in Nox1-Deficient Mice

Kuniharu Matsuno, MS; Hiroyuki Yamada, MD, PhD; Kazumi Iwata, MS; Denan Jin, MD, PhD; Masato Katsuyama, PhD; Masato Matsuki, MD, PhD; Shinji Takai, PhD; Kiyofumi Yamanishi, MD, PhD; Mizuo Miyazaki, MD, PhD; Hiroaki Matsubara, MD, PhD; Chihiro Yabe-Nishimura, MD, PhD

Background—Increased production of reactive oxygen species (ROSs) by angiotensin II (Ang II) is involved in the initiation and progression of cardiovascular diseases. NADPH oxidase is a major source of superoxide generated in vascular tissues. Although Nox1 has been identified in vascular smooth muscle cells as a new homolog of gp91phox (Nox2), a catalytic subunit of NADPH oxidase, the pathophysiological function of Nox1-derived ROSs has not been fully elucidated. To clarify the role of Nox1 in Ang II–mediated hypertension, we generated Nox1-deficient ($^{-/Y}$) mice.

Methods and Results—No difference in the baseline blood pressure was observed between Nox1$^{+/Y}$ and Nox1$^{-/Y}$. Infusion of Ang II induced a significant increase in mean blood pressure, accompanied by augmented expression of Nox1 mRNA and superoxide production in the aorta of Nox1$^{+/Y}$, whereas the elevation in blood pressure and production of superoxide were significantly blunted in Nox1$^{-/Y}$. Conversely, the infusion of pressor as well as subpressor doses of Ang II did elicit marked hypertrophy in the thoracic aorta of Nox1$^{-/Y}$ similar to Nox1$^{+/Y}$. Administration of a nitric oxide synthase inhibitor (L-NAME) to Nox1$^{+/Y}$ did not affect the Ang II–mediated increase in blood pressure, but it abolished the suppressed pressor response to Ang II in Nox1$^{-/Y}$. Finally, endothelium-dependent relaxation and the level of cGMP in the isolated aorta were preserved in Nox1$^{-/Y}$ infused with Ang II.

Conclusions—A pivotal role for ROSs derived from Nox1/NADPH oxidase was suggested in the pressor response to Ang II by reducing the bioavailability of nitric oxide. (***Circulation.*** **2005;112:2677-2685.)**

Key Words: angiotensin ■ aorta ■ hypertension ■ hypertrophy ■ nitric oxide

Accumulating evidence indicates that angiotensin (Ang) II, the principal effector peptide of the renin-angiotensin system, plays a major role in the initiation and progression of such vascular diseases as hypertension, vascular hypertrophy, and atherosclerosis.[1] These effects of Ang II are mediated by reactive oxygen species (ROSs) generated by membrane-bound nicotinamide adenine dinucleotide phosphate (NADPH) oxidase localized in the vascular wall.[2,3] The ROSs originating from the vascular oxidase have been held responsible for endothelial dysfunction and also recognized as important signaling molecules involved in vascular remodeling.[4]

Editorial p 2585
Clinical Perspective p 2685

Early studies on the source of oxidant generation were typically limited to the prototypical NADPH oxidase of phagocytic cells, which is a multisubunit enzyme comprising a membrane-associated cytochrome b_{558} (a heterodimer of a catalytic subunit gp91phox and p22phox) and several cytosolic regulatory subunits (p47phox, p40phox, p67phox, and Rac1 or Rac2). In recent years, 4 homologs of gp91phox (Nox2), named Nox1,[5] Nox3, Nox4, and Nox5,[6] have been identified as components of nonphagocyte-type NADPH oxidase. Among these Nox isoforms expressed primarily in nonphagocyte cells, Nox1 is highly expressed in colon epithelial cells.[5] In vessels, Nox1 mRNA has been detected in vascular smooth muscle cells (VSMCs) and endothelial cells but not in adventitial cells. Conversely, the phagocyte-type subunit Nox2 is localized primarily in endothelial and adventitial cells, whereas Nox4 is abundantly expressed in all of the vessel constituents.[7–11]

Although genetic approaches have been used in recent investigations, there is a relative paucity of information on the role of Nox isoforms in Ang II–mediated vascular disor-

Received July 6, 2005; revision received August 17, 2005; accepted August 18, 2005.

From the Department of Pharmacology (K.M., K.I., M.K., C.Y.-N.), Department of Cardiovascular Medicine (H.Y., H.M.), and Department of Dermatology (M. Matsuki, K.Y.), Kyoto Prefectural University of Medicine, Kyoto; and the Department of Pharmacology, Osaka Medical College (D.J., S.T., M. Miyazaki), Osaka, Japan. Drs Matsuki and Yamanishi are now at the Department of Dermatology, Hyogo College of Medicine, Nishinomiya, Japan.

The online-only Data Supplement, which contains a table, can be found at http://circ.ahajournals.org/cgi/content/full/CIRCULATIONAHA.105.573709/DC1.

Correspondence to Chihiro Yabe-Nishimura, MD, PhD, Department of Pharmacology, Kyoto Prefectural University of Medicine, Kyoto 602-8566, Japan. E-mail nchihiro@koto.kpu-m.ac.jp

Circulation **is available at http://www.circulationaha.org** **DOI: 10.1161/CIRCULATIONAHA.105.573709**

ders.[12–14] In knockout mice genetically deficient in Nox2, the basal blood pressure was lower than wild-type counterparts, whereas Ang II–dependent hypertension was unaffected.[14,15] In the aortic media of these knockout mice, hypertrophic responses to Ang II infusion were significantly attenuated.[14] Conversely, the hypertensive response to Ang II was significantly reduced in knockout mice of p47phox, a regulatory subunit of NADPH oxidase.[16] These results suggest that Nox1 may participate in Ang II–induced hypertension, because p47phox can regulate both Nox2 and Nox1.[17] To clarify the role of the Nox1 isoform in the pathogenesis of Ang II–induced hypertension, we generated Nox1-deficient mice and administered Ang II by osmotic minipumps. We report here results indicating a pivotal role for Nox1/NADPH oxidase in the pressor response to Ang II.

Methods

Generation of Nox1-Deficient Mice

Mouse genomic clones containing the *Nox1* locus were isolated from a 129/SvJ mouse genomic library constructed in lambda FixII (Stratagene) using a murine Nox1 partial cDNA fragment as a probe. A 6.5-kb *Sac*I-*Hin*dIII fragment and a 1.0-kb *Hin*dIII-*Bam*HI fragment were cloned into pBluescript II-KS (+), a plasmid containing a neomycin (neo) expression cassette driven by the murine phosphoglycerate kinase promoter. At the 3′ end of the vector, a diphtheria toxin A fragment was included to serve as a negative selection marker. The Nox1 targeting vector was designed to replace the 1.5 kb of the genomic locus containing exon 3 to 6 with the neo cassette.

R1 embryonic stem (ES) cells were transfected with the linearized targeting vector and selected with G418. Targeted ES clones were identified by polymerase chain reaction (PCR) screening and verified by Southern hybridization using genomic probes located on the 5′ and 3′ sides of the Nox1 gene. Correctly targeted ES cells were used to make chimeric mice by aggregating the cells in E2.5 embryos and transferring the aggregated embryos to pseudopregnant females.[18] Male chimeras were crossed with C57BL/6 females to generate heterozygous mice. Heterozygous females were crossed with C57BL/6 males to obtain Nox1-deficient mice ($Nox1^{-/Y}$). The present study was performed with the approval of the Committee for Animal Research at Kyoto Prefectural University of Medicine.

Animal Model

Nox1-deficient mice and their control littermates (8 to 12 weeks old) were anesthetized with sodium pentobarbital (80 mg/kg IP). The intrascapular region was shaved, and an osmotic minipump (Alzet model 2002; Durect Corp) that contained [Val^5] angiotensin II (Sigma) or vehicle (phosphate-buffered saline, PBS) was inserted to permit subcutaneous infusion of Ang II (0.7 mg · kg^{-1} · d^{-1}). In an additional series of experiments, a subpressor dose of Ang II (0.14 mg · kg^{-1} · d^{-1}) was administered for 28 days to induce vascular hypertrophy by use of osmotic minipumps (Alzet model 2004). N^G-Nitro-L-arginine methyl ester (L-NAME) purchased from Nacalai Tesque was administered in the drinking water for 14 days (1.4 mg/d).

DHE Staining

On day 7 of Ang II administration, the thoracic aorta was dissected and snap-frozen in liquid nitrogen after being embedded in Tissue-Tek O.C.T. compound (Sakura Finetechnical Co). Unfixed frozen ring segments were cut into 30-μm-thick sections and placed on a glass slide. Dihydroethidium (DHE, 10 μmol/L, Molecular Probes) was topically applied to each tissue section and coverslipped. Slides were incubated in a light-protected humidified chamber at 37°C for 30 minutes. For the detection of ethidium bromide, a 543-nm He-Ne laser combined with a 560-nm long-pass filter was used.

Detection of Superoxide Production

Superoxide (O_2^-) production was measured with the L-012 chemiluminescence assay as described previously.[19] L-012 (Wako Pure Chemical Industries, Ltd) is a luminol derivative with high sensitivity to superoxide radicals that does not exert redox cycling itself.[20] After the infusion of Ang II for 7 days, aortic rings (0.5 cm) were dissected and incubated for 30 minutes in Krebs-HEPES buffer at 37°C. Rings were transferred to scintillation vials containing 100 μmol/L L-012 in Krebs-HEPES buffer and incubated for 5 minutes at 37°C in the dark. After incubation, chemiluminescence was measured by luminometer (Lumat LB 9507, Berthold Technologies Ltd) over a period of 10 minutes at 1-minute intervals. The L-012 chemiluminescence was expressed as relative light units per milligram of dry tissue weight per minute.

Blood Pressure and Heart Rate Measurements

Blood pressure and heart rate in conscious mice were measured by the tail-cuff system using BP98A (Softron Co). Before the osmotic pump was implanted, at least 3 days of training were conducted to accustom mice to the procedure. For each time point, 5 measurements were obtained and averaged for each mouse. Mean blood pressure (MBP) was used for all data analysis.

Real-Time PCR

The thoracic aorta of mice was dissected and snap-frozen in liquid nitrogen. Total RNA was isolated by the acid guanidinium thiocyanate/phenol/chloroform method. Real-time PCR was performed by use of the GeneAmp 5700 Sequence Detection System (Applied Biosystems) with the SuperScript III Platinum SYBR Green One-Step qRT-PCR Kit (Invitrogen Corp). The primer sequences used are shown in the Data Supplement Table (http://circ.ahajournals.org/cgi/content/full/CIRCULATIONAHA.105.573709/DC1). Dissociation curves were monitored to check the aberrant formation of primer dimers. PCR-amplified products were electrophoresed on 2% agarose gels to confirm the presence of a single band. Copy numbers were calculated on the basis of standard curves generated with genuine Nox1, Nox2, and Nox4 cDNA templates. Data were expressed as copies per microgram RNA or levels relative to day 0 (%).

Histological Analysis

After the infusion of Ang II, mice were anesthetized and perfused transcardially with 10 mL of PBS followed by 10 mL of 4% paraformaldehyde phosphate buffer under pressure (100 mm Hg). The aorta, placed in 4% formalin overnight, was processed and embedded in paraffin. Three sections (6 μm) were obtained from each descending thoracic aorta, 3 mm distal to the left subclavian artery at 500-μm intervals, and stained with elastica van Gieson stain. The medial areas and circumference of the external elastic lamina were measured by use of ImageJ software. The medial thickness was calculated by dividing the medial area by the circumference of the external elastic lamina.

Measurement of cGMP Levels

After the infusion of Ang II for 7 days, the thoracic aorta was dissected and connective tissue was removed. Vessels were immediately snap-frozen in liquid nitrogen and homogenized in ice-cold 5% trichloroacetic acid. The level of cGMP in the supernatant fraction of the homogenate was measured by an enzyme immunoassay (Cayman Chemical Co) and expressed as picomoles per milligram of the dry trichloroacetic acid precipitate.

Isolated Vascular Strip Experiments

Endothelium-dependent and -independent relaxations of the isolated vessels were measured in ex vivo organ chamber baths as described previously.[21] Briefly, after the infusion of Ang II for 7 days, mice were anesthetized, and thoracic aorta was dissected free from surrounding connective tissue. The aorta was cut into helical strips (10 mm long and 1 mm wide). The resting tension was adjusted to 0.2 g, which is optimal for induction of a maximal contraction. The strips were equilibrated for 90 minutes in organ baths containing Tyrode's solution. After equilibration, the strips were precontracted

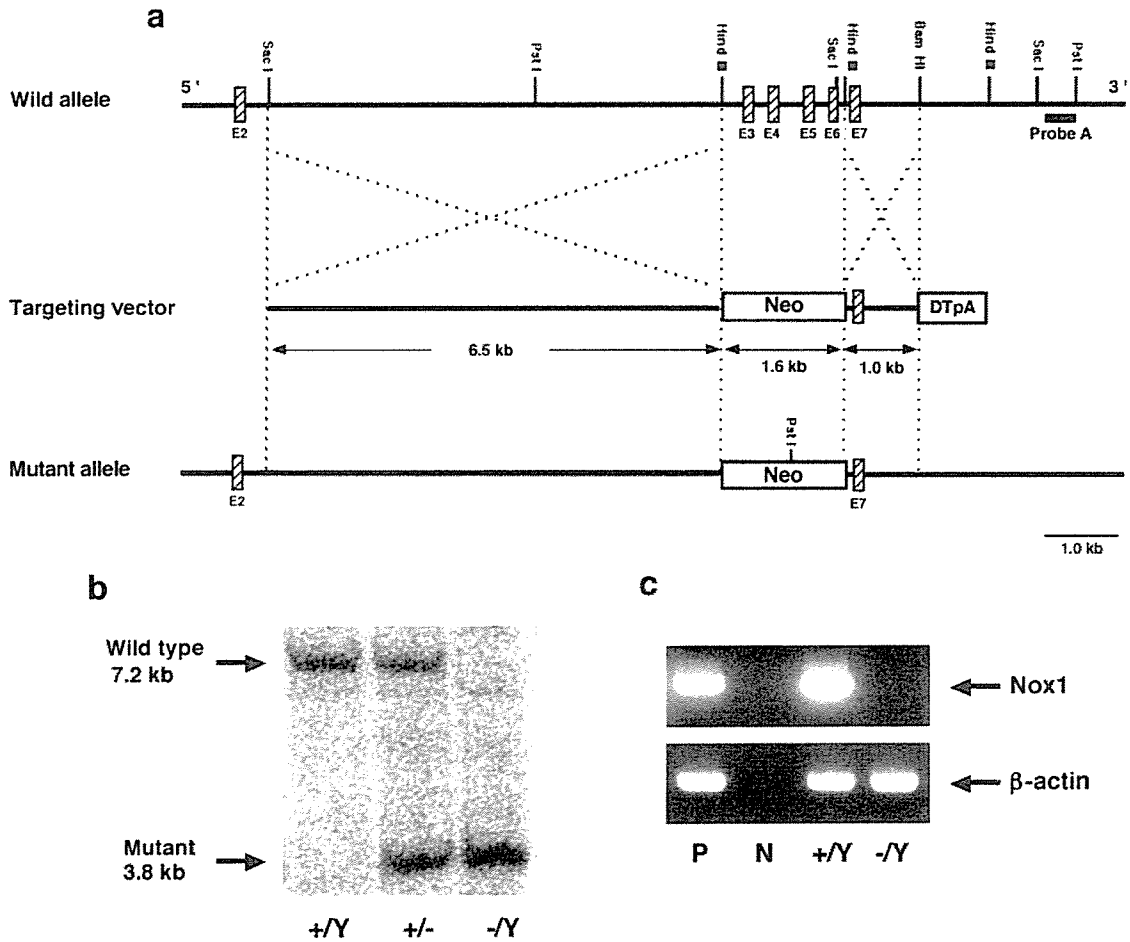

Figure 1. Targeted disruption of the mouse Nox1 gene. a, Diagram of the targeting vector (middle) designed to replace the *Hin*dIII fragment containing exon 3 to exon 6 of the Nox1 gene in the wild-type allele (top) with a pGK-neo cassette (Neo). The predicted mutant allele generated by homologous recombination is shown (bottom). b, Southern blot analysis to verify the homologous recombination. The genomic DNAs obtained from F2 offspring (+/Y, wild-type; +/−, hetero; −/Y, knockout) were digested with *Pst*I and hybridized with probe A, marked as a solid bar in a, located downstream of the targeted region. Bands corresponding to the wild-type allele (7.2 kb) and mutant allele (3.8 kb) are indicated. c, Reverse transcription–PCR of Nox1 mRNA in the colon. Ethidium bromide staining of the products corresponding to the Nox1 transcript (top) and β-actin (bottom). P indicates positive control (mouse colon); N, negative control (no template).

with norepinephrine (30 nmol/L, Sankyo Co). At the maximal constriction level, acetylcholine (ACh, Daiichi Pharmaceutical Co) or sodium pentacyanonitrosylferrate dihydrate (Nacalai Tesque, Kyoto, Japan) was added to evaluate vasodilator function. After a stable relaxation was achieved with ACh, papaverine (100 μmol/L, Sanko Seiyaku Kogyo Co) was added to induce a maximal relaxation. Relaxation was assessed by percent relaxation relative to papaverine-mediated relaxation (100%).

Statistics

The results are expressed as the mean±SEM. For multiple treatment groups, repeated-measures, 2-way, or Latin-square design ANOVA followed by a Tukey-Kramer test was applied. For expression levels of Nox isoforms, a Kruskal-Wallis test was performed, followed by a Dunnett test.

Results

Generation of Nox1-Deficient Mice

Nox1-deficient mice were generated by replacing exon 3 to 6 containing presumed membrane-spanning regions with the neo cassette (Figure 1a). Two independent ES clones yielded germ-line chimeras and their heterozygous mutant F1 mice. Because the locus of the Nox1 gene is on the X chromosome, heterozygotes obtained at F1 generation were female. The heterozygous females were crossed with C57BL/6 males to obtain Nox1-deficient ($^{-/Y}$) mice. The ratio of genotypes of the offspring did not deviate significantly from the expected 1:1 distribution of male Nox1$^{+/Y}$ and Nox1$^{-/Y}$ offspring. Southern blot analysis of the *Pst*I-digested genomic DNA obtained from F2 offspring demonstrated a 7.2-kb band for the wild-type allele and a 3.8-kb band for the mutant allele (Figure 1b). Because mouse Nox1 mRNA is most abundantly expressed in the colon,[5] we verified the expression of Nox1 mRNA in the colon. Although a 902-base band was clearly detected in Nox1$^{+/Y}$ by reverse transcription–PCR, Nox1 mRNA was absent in Nox1$^{-/Y}$ (Figure 1c). Compared with their control littermates, Nox1$^{-/Y}$ grew with normal weight gain and without obvious abnormalities in their general appearance.

Ang II–Induced Superoxide Production Was Reduced in Nox1-Deficient Mice

The effect of Nox1 gene disruption on vascular superoxide production was first investigated by DHE staining of the frozen

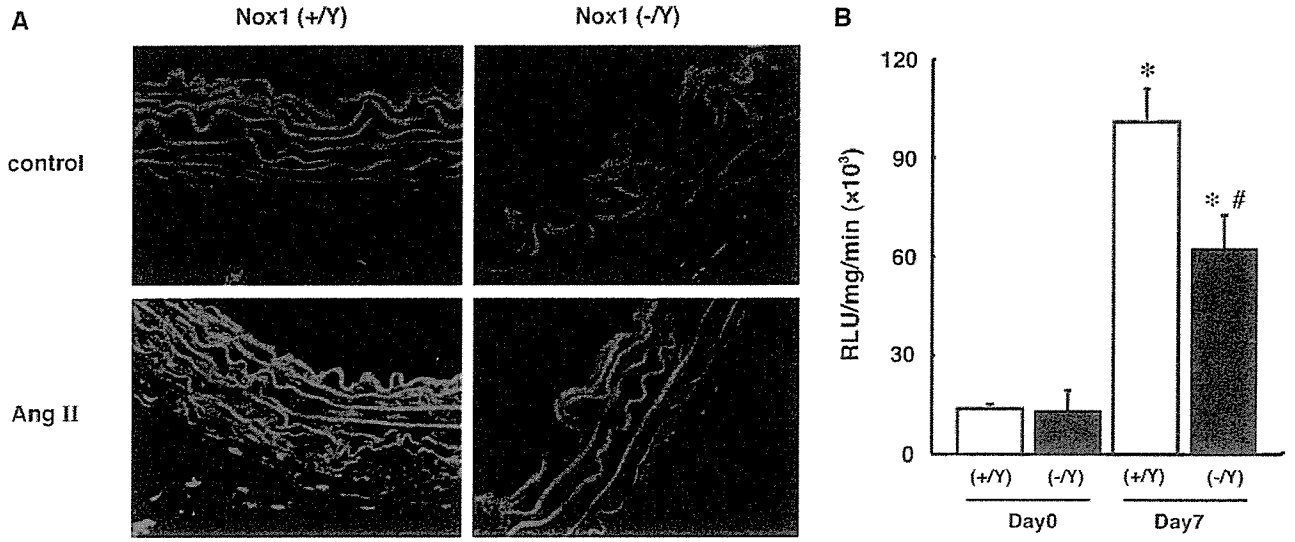

Figure 2. Superoxide production in the thoracic aorta of mice infused with Ang II. A, In situ detection of superoxide production with dihydroethidium (DHE). Cross sections of the thoracic aorta were obtained from mice infused with Ang II (0.7 mg · kg^{-1} · d^{-1}) or vehicle for 7 days. Each image is representative of the results from 3 animals. B, Levels of superoxide in thoracic aortae of mice infused with Ang II or vehicle for 7 days were determined by L-012 chemiluminescence. N=3 to 4 per group. *P<0.05 vs corresponding day 0 group. #P<0.05 vs corresponding Nox1$^{+/Y}$.

sections of the aorta (Figure 2A). A low level of DHE fluorescence was detected in the thoracic aorta of Nox1$^{+/Y}$ or Nox1$^{-/Y}$ after PBS infusion for 7 days. Infusion of Ang II for 7 days markedly increased DHE fluorescence in Nox1$^{+/Y}$ aorta throughout the vessel wall. Conversely, DHE fluorescence in Ang II–treated Nox1$^{-/Y}$ was significantly attenuated in the media.

We next performed the L-012 chemiluminescence assay. No difference in L-012 chemiluminescence was detected in the thoracic aorta of Nox1$^{+/Y}$ or Nox1$^{-/Y}$ after the infusion of PBS for 7 days. In Ang II–infused mice, the chemiluminescence of the aorta was significantly less intense in Nox1$^{-/Y}$ than Nox1$^{+/Y}$ (Figure 2B).

Pressor Response to Ang II Was Suppressed in Nox1-Deficient Mice

Between the age-matched Nox1$^{+/Y}$ and Nox1$^{-/Y}$ mice, no difference in initial body weight was observed. There was no difference in the baseline MBP determined between these experimental groups. In response to continuous infusion of 0.7 mg · kg^{-1} · d^{-1} of Ang II, MBP levels were similarly elevated in both Nox1$^{+/Y}$ and Nox1$^{-/Y}$ until day 5 of treatment. On day 7 of the infusion, however, the increase was significantly suppressed, and a lower MBP was demonstrated in Nox1$^{-/Y}$ compared with Nox1$^{+/Y}$ until day 14 of infusion (Figure 3). Conversely, there was no difference in the basal heart rate between Nox1$^{+/Y}$ and Nox1$^{-/Y}$ (+/Y, 605.3±24.8 versus −/Y, 602.0±25.1 bpm, N=8 to 9). No difference in heart rate of Ang II–infused mice was observed between these groups on day 14 (+/Y, 598.2±18.8 versus −/Y, 599.0±22.0, N=8 to 9).

Ang II–Upregulated Expression of Nox Isoforms in the Aorta

The Ang II–induced elevation in MBP was blunted in Nox1$^{-/Y}$ at 7 days of treatment. We therefore investigated expression levels of Nox1, Nox2, and Nox4 mRNA in the thoracic aorta of mice treated with Ang II. As shown in Figure 4a, Nox1 mRNA levels in Nox1$^{+/Y}$ significantly increased on day 7, and increased levels were sustained during the course of Ang II infusion. A concomitant increase in Nox2 mRNA level was demonstrated on day 5, which returned to the basal level on day 14 (Figure 4b). Conversely, increased Nox4 mRNA levels were observed on days 7 and 14 of Ang II infusion (Figure 4c). In Nox1$^{-/Y}$ mice, similar increases in Nox2 and Nox4 mRNAs were demonstrated at 0, 7, and 14 days of treatment (Figure 4d).

Nox1 Was Not Involved in the Ang II–Induced Vascular Hypertrophy

We previously reported the involvement of Nox1 in prostaglandin $F_{2\alpha}$ ($PGF_{2\alpha}$)–induced hypertrophy of VSMCs in culture.[22] Because vascular hypertrophy is closely linked to elevated blood pressure, we investigated the effect of Ang II

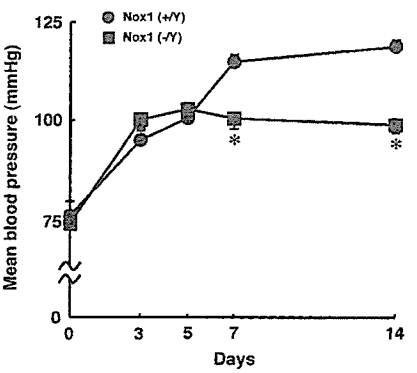

Figure 3. Changes in blood pressure during Ang II infusion. MBP was determined with the tail-cuff system as described in Methods. Ang II was continuously infused with an osmotic pump. N=8 to 9 per group. *P<0.05 vs corresponding Nox1$^{+/Y}$.

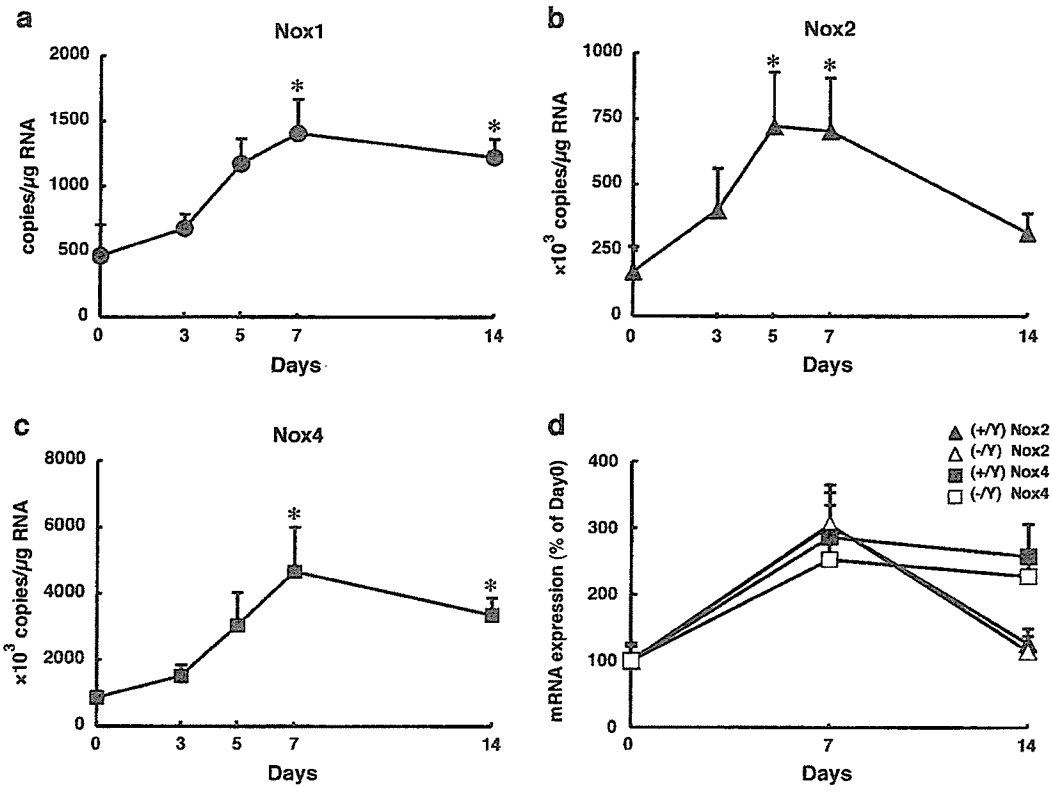

Figure 4. Expression of Nox1 and other Nox isoforms during Ang II infusion. a–c, Time course of expression of Nox isoforms in Nox1$^{+/Y}$. Total RNA was isolated from the thoracic aorta at the indicated day of Ang II infusion. Nox1, Nox2, and Nox4 mRNAs were detected by real-time PCR. Data are expressed as copies per microgram RNA. N=5 per group. *P<0.05 vs day 0. d, Relative mRNA levels of Nox isoforms in Nox1$^{+/Y}$ and Nox1$^{-/Y}$. Data are expressed as levels relative to day 0 (%). N=5 to 7 per group.

infusion on the vascular architecture in Nox1$^{-/Y}$. When medial area and thickness in cross sections of the thoracic aorta were compared, the infusion of Ang II for 14 days was found to have induced significant hypertrophy in both Nox1$^{+/Y}$ and Nox1$^{-/Y}$ (Figure 5a). Contrary to the results of in vitro studies, medial area and thickness of Nox1$^{-/Y}$ were markedly increased, similar to those of Nox1$^{+/Y}$ (Figure 5b). No change in these parameters was observed in control mice infused with vehicle (PBS) for 14 days.

We further investigated the effect of a subpressor dose of Ang II (0.14 mg · kg^{-1} · d^{-1}) in Nox1-deficient mice. As shown in Figure 5c, no change in MBP was observed in mice infused with a subpressor dose of Ang II for 28 days. Under equivalent blood pressure conditions, significant hypertrophy in the media was observed in both Nox1$^{+/Y}$ and Nox1$^{-/Y}$. Medial area and thickness of the thoracic aorta increased in Nox1$^{-/Y}$ to an extent similar to that in Nox1$^{+/Y}$.

L-NAME Abolished the Suppression of Pressor Response to Ang II in Nox1-Deficient Mice

In Ang II–induced hypertension, superoxide derived from vascular NADPH oxidase has been reported to impair endothelium-dependent relaxation by inactivating nitric oxide (NO), an endothelial vasodilator. To investigate the possible interaction between Nox1 deficiency and endogenous NO, we administered 1.4 mg/d of L-NAME, an NO synthase inhibitor, to Nox1$^{+/Y}$ and Nox1$^{-/Y}$ (Figure 6A). Administration of L-NAME for 14 days slightly elevated basal MBP levels in Nox1$^{+/Y}$ and Nox1$^{-/Y}$, although the effect was statistically insignificant. The pressor response to Ang II in Nox1$^{+/Y}$ was unaffected by L-NAME, whereas in Ang II–infused Nox1$^{-/Y}$, MBP was significantly elevated by administration of L-NAME. Consequently, no difference in MBP levels was observed between Nox1$^{+/Y}$ and Nox1$^{-/Y}$ treated with Ang II along with L-NAME.

cGMP Level in the Aorta Was Preserved in Nox1-Deficient Mice Infused With Ang II

To evaluate the effect of disruption of Nox1/NADPH oxidase on NO bioactivity, we measured the level of cGMP in the thoracic aorta. As shown in Figure 6B, no difference in cGMP levels was observed between Nox1$^{+/Y}$ and Nox1$^{-/Y}$ infused with vehicle (PBS) for 7 days. In Ang II–infused mice, conversely, cGMP levels were significantly decreased in Nox1$^{+/Y}$, whereas the levels in Nox1$^{-/Y}$ were retained. No difference in the activity of NO synthase was demonstrated between Nox1$^{+/Y}$ and Nox1$^{-/Y}$ treated with Ang II (data not shown).

Endothelium-Dependent Vasodilatation Was Preserved in Nox1-Deficient Mice Infused With Ang II

Finally, vascular relaxations in aortic strips were studied to determine whether Nox1-derived ROSs are involved in the

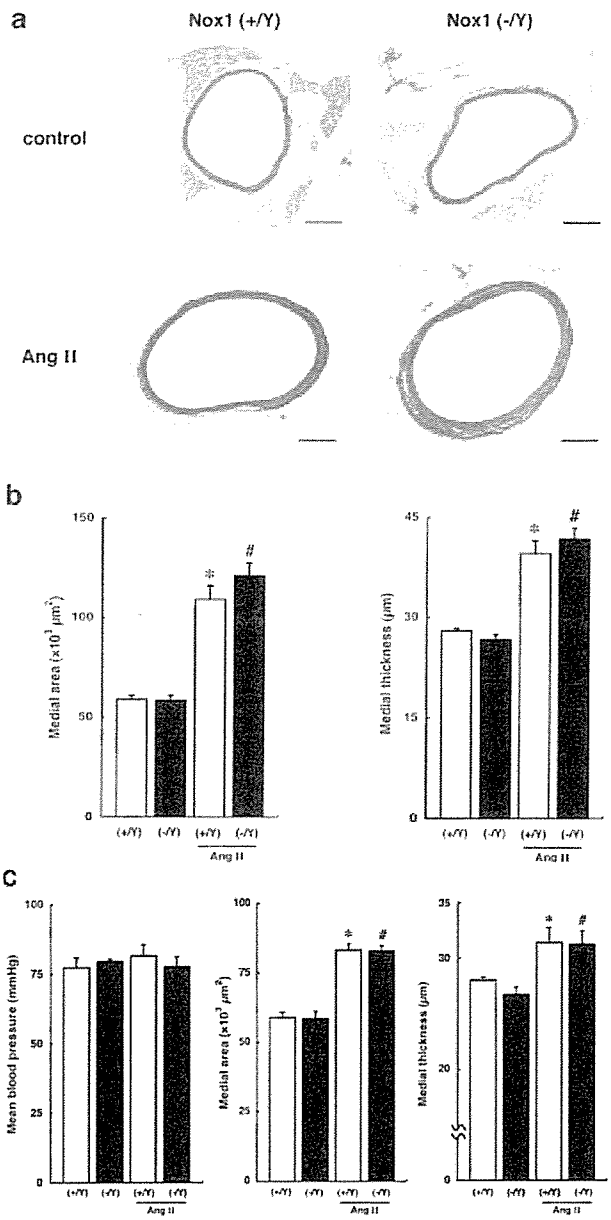

Figure 5. Histological analysis of the thoracic aorta of mice infused with Ang II. a, Representative cross sections of the thoracic aorta stained with elastica van Gieson stain. Scale bar=200 μm. b, Quantitative analyses of medial area (left) and thickness (right). Ang II (0.7 mg · kg^{-1} · d^{-1}) or vehicle was infused for 14 days. N=5 to 6 per group. *P<0.05, #P<0.05 vs corresponding vehicle-treated group. c, Effects of a subpressor dose of Ang II infusion. Ang II (0.14 mg · kg^{-1} · d^{-1}) or vehicle was continuously infused with an osmotic pump for 28 days, when MBP (left), medial area (middle), and thickness (right) were determined. N=5 to 6 per group. *P<0.05, #P<0.05 vs corresponding vehicle-treated group.

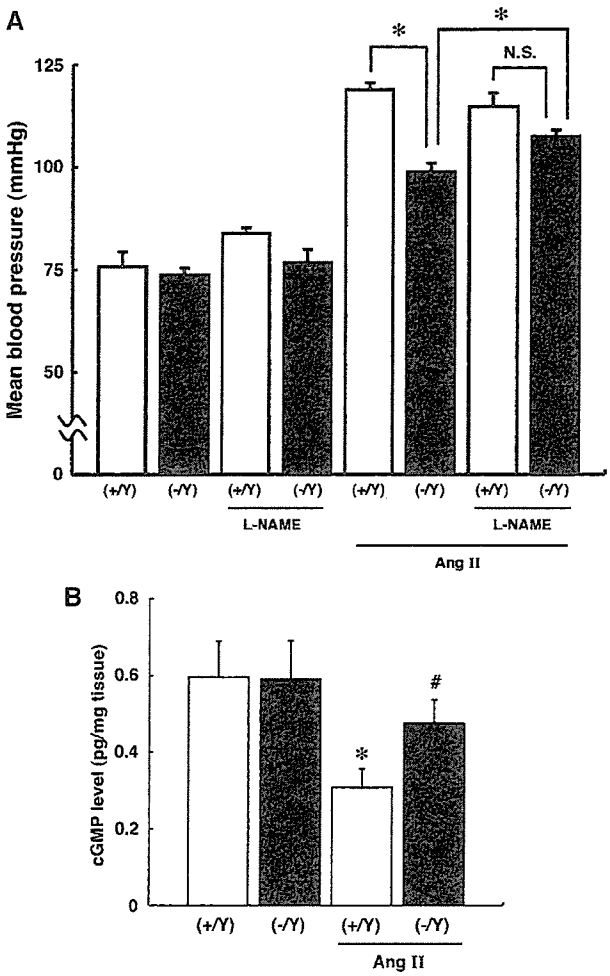

Figure 6. NO signaling in Ang II–infused mice. A, Effects of L-NAME on pressor response to Ang II. Reduced pressor response to Ang II in Nox1$^{-/Y}$ was abolished by administration of L-NAME (1.4 mg/d). MBP was determined on day 14 of vehicle or Ang II infusion. N=5 to 9 per group. *P<0.05; N.S., not significant. B, Aortic cGMP level. cGMP levels in thoracic aortae of mice infused with Ang II or vehicle for 7 days were measured by an enzyme immunoassay. N=7 to 11 per group. *P<0.05 vs vehicle-treated Nox1$^{+/Y}$. #P<0.05 vs Ang II–infused Nox1$^{+/Y}$.

Ang II–induced alteration in vascular reactivity. In the vehicle-infused Nox1$^{-/Y}$, the response to ACh was slightly better than that in Nox1$^{+/Y}$, without statistical significance (Figure 7a). After the infusion of Ang II for 7 days, the response to ACh was significantly attenuated in Nox1$^{+/Y}$. In contrast, Ang II infusion did not affect the ACh-induced relaxation in Nox1$^{-/Y}$. As shown in Figure 7b, endothelium-independent relaxations to sodium pentacyanonitrosylferrate dihydrate were similar in aortic strips obtained from all experimental groups. Usage of $PGF_{2\alpha}$ as an alternative contractile substance gave similar results, and no difference in the contractile response to norepinephrine or Ang II was observed between Nox1$^{+/Y}$ and Nox1$^{-/Y}$ infused with vehicle or Ang II (data not shown). These findings suggest that scavenging of NO by Nox1-derived ROSs underlies the development of Ang II–induced hypertension.

Discussion

In this study, we clarified for the first time the role of Nox1 in the pathogenesis of Ang II–mediated hypertension using Nox1-deficient mice. The principal findings obtained were that ROSs derived from Nox1/NADPH oxidase are crucial to

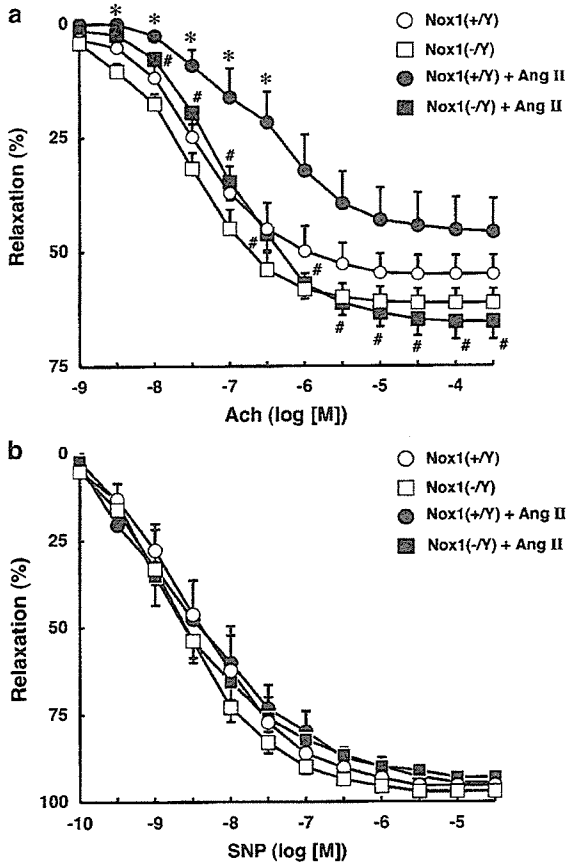

Figure 7. Vascular relaxations in Ang II–infused mice. After the infusion of vehicle or Ang II for 7 days, vascular reactivity to endothelium-dependent agonist ACh (a) or endothelium-independent NO donor sodium pentacyanonitrosylferrate dihydrate (SNP) (b) was measured in isolated aortic strips. N=4 to 6 per group. *$P<0.05$ vs vehicle-treated Nox1$^{+/Y}$. #$P<0.05$ vs Ang II–infused Nox1$^{+/Y}$.

the pressor response to Ang II by reducing the bioavailability of NO.

The present findings suggest that Nox1 is involved in the late phase but not in the early phase of the pressor response to Ang II. In both Nox1$^{+/Y}$ and Nox1$^{-/Y}$, MBP was increased up to day 5 of Ang II infusion, whereas in Nox1$^{-/Y}$, the pressor response was blunted after 7 days. Meanwhile, Nox1 mRNA expression was markedly upregulated from day 7 in Nox1$^{+/Y}$. Vascular superoxide production is known to impair vascular relaxation through the inactivation of endothelial NO, which serves as an important component in the development and maintenance of increased blood pressure.[23] It has been reported that administration of tempol, a superoxide dismutase mimetic, abolishes the pressor response to Ang II.[24] We also observed that administration of tempol almost completely abolished the pressor response to Ang II in both Nox1$^{+/Y}$ and Nox1$^{-/Y}$ (data not shown). It therefore seems likely that ROSs derived from another source participate in the early phase of the pressor response to Ang II. In the present Ang II–treated mice, a marked increase in Nox2 mRNA in the aorta was demonstrated at day 5 and 7. In a previous study using Nox2-deficient mice, however, infusion of Ang II for 6 days caused an increase in systolic blood pressure similar to that in wild-type mice.[14] A recent study also reported that inactivation of Nox2 had no effect on the development of hypertension in a model in which the endogenous renin-angiotensin system is chronically upregulated.[15] These findings therefore suggest that Nox2 does not participate in the late phase of the hypertensive response to Ang II in a murine animal model. Meanwhile, a gradual increase in Nox4 mRNA was observed during Ang II infusion, but the level was unchanged at day 3, when the early phase of the pressor response was already depicted. Although the source of ROSs responsible for the early phase of increased MBP in Ang II–infused Nox1$^{-/Y}$ is still unclear, an alternative possibility may be that a rapid increase in superoxide production by activated Nox2 or Nox4/NADPH oxidase takes part in the early phase of the hypertensive response in Nox1$^{-/Y}$. Ang II–induced production of ROSs by NADPH oxidase is known to take place instantly, which depends on the activation of protein kinase C and a small G protein, Rac.[25]

Ang II induces vascular hypertrophy, and it is well known that vascular hypertrophy is closely linked to elevation in blood pressure. We previously demonstrated that depletion of Nox1 mRNA by ribozymes significantly reduced the increased protein synthesis induced by $PGF_{2\alpha}$ in a rat VSMC-derived cell line.[22] Nox1 in fact mediates Ang II–induced activation of the redox-sensitive signaling molecules, p38 mitogen-activated protein kinase and Akt, both of which are required for hypertrophy of VSMCs.[12] However, our study demonstrated that hypertrophic responses to pressor and subpressor doses of Ang II in Nox1$^{-/Y}$ were similar to those in Nox1$^{+/Y}$. These findings clearly indicate that Nox1 is not associated with the development of vascular hypertrophy induced by Ang II, which is inconsistent with the previous studies in vitro. Why such inconsistent findings have come about is a subject for further investigation. Under conditions in vivo, however, the ROSs responsible for vascular hypertrophy may derive primarily from Nox2 localized in the endothelial and adventitial cells. ROSs derived from Nox1 may have a limited effect because of its low level of activity compared with that of Nox2.[4] Because such growth-promoting ROSs as hydrogen peroxide diffuse freely across the cell membrane, VSMCs in Ang II–infused Nox1$^{-/Y}$ may yet be exposed to a high level of ambient ROSs, whereas isolated VSMCs in culture are unaffected by Nox2-derived ROSs. Also to be considered is the fact that VSMCs removed from their tissue of origin and placed in cell culture transform from a contractile to a synthetic phenotype.[26] In vascular injury and atherosclerosis, VSMCs also transform from a contractile to a synthetic phenotype.[27,28] Although hypertrophy in the aorta of Ang II–infused mice developed in the absence of Nox1, the findings in cell culture suggest that Nox1 may be involved in vascular remodeling under different experimental or pathological conditions.

Administration of L-NAME abolished the effect of Nox1 gene disruption on the pressor response to Ang II, whereas the level of cGMP, a second messenger of the NO signaling cascade, was preserved in Ang II–infused Nox1$^{-/Y}$ vessels. It

has been generally accepted that ROSs decrease the bioavailability of NO by scavenging NO and causing endothelial NO synthase uncoupling, thereby contributing to the pathogenesis of hypertension.[29] Uncoupling of endothelial NO synthase appears not to be involved in the pressor response to Ang II under our experimental conditions, because pretreatment with L-NAME did not affect superoxide production in aortic rings isolated from Ang II–treated mice (data not shown). Our findings thus suggest that the preservation of the availability of NO through depletion of Nox1-derived ROSs is the underlying mechanism of the suppressed pressor response in Nox1$^{-/Y}$. The fact that endothelium-dependent vascular relaxation was maintained in Ang II–infused Nox1$^{-/Y}$ aorta further strengthens this view.

It should be noted that Nox1-derived ROSs participated primarily in the pressor response to Ang II, although an Ang II–induced increase in superoxide production could be attributed to augmented expression of Nox2 and Nox4 in the vascular wall as well. In the thoracic aorta, quantitative determination of mRNA levels illustrated dominant expression of Nox2 and Nox4 compared with Nox1. However, superoxide production in isolated aorta was significantly attenuated in Ang II–infused Nox1$^{-/Y}$. Such a discrepancy in the levels of Nox transcripts expressed in the aorta and their relative contribution to superoxide production may be explained by distribution and interaction of these catalytic subunits with other subunits required for full enzyme activity.[23] ROSs generated by NADPH oxidase act as intracellular and intercellular signaling molecules,[12] and Nox1-derived ROSs in the kidney may also participate in the regulation of the pressor response to Ang II.[30] In this context, multiple sites of action may be involved in the antihypertensive response in Nox1$^{-/Y}$.

To date, no isoform-specific inhibitors of the Nox family have been developed. Knockout mice are therefore important tools with which to clarify the functional roles of Nox isoforms in vivo. A previous report using Nox2-deficient mice demonstrated the involvement of Nox2 in the regulation of the basal blood pressure and in Ang II–induced vascular hypertrophy but not in the pressor response to Ang II.[14,15] Taking these findings into consideration, it is notable that each Nox isoform plays a distinct role in the development of vascular disorders. Isoform-specific inhibitors of the Nox family may therefore become ideal therapeutic agents for the treatment of vascular disorders with diverse pathological backgrounds.

Acknowledgments

We thank Dr N. Urao of the Department of Cardiovascular Medicine and Drs T. Nishinaka, M. Ibi, and N. Arakawa of the Department of Pharmacology for valuable discussion and advice. We are also grateful to Drs T. Aihara, K. Amagase, and E. Nakamura of the Department of Applied Pharmacology, Kyoto Pharmaceutical University, for valuable advice and assistance. The authors are indebted to Dr J. Takeda of the Department of Social and Environmental Medicine, Osaka University, for initial guidance with the gene targeting study. This work was supported in part by a Grant-in-Aid for Young Scientists (B) 16790310 (to K. Iwata) and 14770036 (to Dr Katsuyama) from the Ministry of Education, Culture, Sports, Science, and Technology of Japan.

References

1. Kim S, Iwao H. Molecular and cellular mechanisms of angiotensin II-mediated cardiovascular and renal diseases. *Pharmacol Rev.* 2000;52:11–34.
2. Griendling KK, Minieri CA, Ollerenshaw JD, Alexander RW. Angiotensin II stimulates NADH and NADPH oxidase activity in cultured vascular smooth muscle cells. *Circ Res.* 1994;74:1141–1148.
3. Zhang H, Schmeisser A, Garlichs CD, Plotze K, Damme U, Mugge A, Daniel WG. Angiotensin II–induced superoxide anion generation in human vascular endothelial cells: role of membrane-bound NADH-/NADPH-oxidases. *Cardiovasc Res.* 1999;44:215–222.
4. Griendling KK, Sorescu D, Ushio-Fukai M. NAD(P)H oxidase: role in cardiovascular biology and disease. *Circ Res.* 2000;86:494–501.
5. Suh YA, Arnold RS, Lassegue B, Shi J, Xu X, Sorescu D, Chung AB, Griendling KK, Lambeth JD. Cell transformation by the superoxide-generating oxidase Mox1. *Nature.* 1999;401:79–82.
6. Lambeth JD. NOX enzymes and the biology of reactive oxygen. *Nat Rev Immunol.* 2004;4:181–189.
7. Ago T, Kitazono T, Ooboshi H, Iyama T, Han YH, Takada J, Wakisaka M, Ibayashi S, Utsumi H, Iida M. Nox4 as the major catalytic component of an endothelial NAD(P)H oxidase. *Circulation.* 2004;109:227–233.
8. Gorlach A, Brandes RP, Nguyen K, Amidi M, Dehghani F, Busse R. A gp91phox containing NADPH oxidase selectively expressed in endothelial cells is a major source of oxygen radical generation in the arterial wall. *Circ Res.* 2000;87:26–32.
9. Pagano PJ, Clark JK, Cifuentes-Pagano ME, Clark SM, Callis GM, Quinn MT. Localization of a constitutively active, phagocyte-like NADPH oxidase in rabbit aortic adventitia: enhancement by angiotensin II. *Proc Natl Acad Sci U S A.* 1997;94:14483–14488.
10. Sorescu GP, Song H, Tressel SL, Hwang J, Dikalov S, Smith DA, Boyd NL, Platt MO, Lassegue B, Griendling KK, Jo H. Bone morphogenic protein 4 produced in endothelial cells by oscillatory shear stress induces monocyte adhesion by stimulating reactive oxygen species production from a nox1-based NADPH oxidase. *Circ Res.* 2004;95:773–779.
11. Szocs K, Lassegue B, Sorescu D, Hilenski LL, Valppu L, Couse TL, Wilcox JN, Quinn MT, Lambeth JD, Griendling KK. Upregulation of Nox-based NAD(P)H oxidases in restenosis after carotid injury. *Arterioscler Thromb Vasc Biol.* 2002;22:21–27.
12. Lassegue B, Sorescu D, Szocs K, Yin Q, Akers M, Zhang Y, Grant SL, Lambeth JD, Griendling KK. Novel gp91(phox) homologues in vascular smooth muscle cells: nox1 mediates angiotensin II–induced superoxide formation and redox-sensitive signaling pathways. *Circ Res.* 2001;88:888–894.
13. Mollnau H, Wendt M, Szocs K, Lassegue B, Schulz E, Oelze M, Li H, Bodenschatz M, August M, Kleschyov AL, Tsilimingas N, Walter U, Forstermann U, Meinertz T, Griendling K, Munzel T. Effects of angiotensin II infusion on the expression and function of NAD(P)H oxidase and components of nitric oxide/cGMP signaling. *Circ Res.* 2002;90:E58–E65.
14. Wang HD, Xu S, Johns DG, Du Y, Quinn MT, Cayatte AJ, Cohen RA. Role of NADPH oxidase in the vascular hypertrophic and oxidative stress response to angiotensin II in mice. *Circ Res.* 2001;88:947–953.
15. Touyz RM, Mercure C, He Y, Javeshghani D, Yao G, Callera GE, Yogi A, Lochard N, Reudelhuber TL. Angiotensin II-dependent chronic hypertension and cardiac hypertrophy are unaffected by gp91phox-containing NADPH oxidase. *Hypertension.* 2005;45:530–537.
16. Landmesser U, Cai H, Dikalov S, McCann L, Hwang J, Jo H, Holland SM, Harrison DG. Role of p47(phox) in vascular oxidative stress and hypertension caused by angiotensin II. *Hypertension.* 2002;40:511–515.
17. Takeya R, Ueno N, Kami K, Taura M, Kohjima M, Izaki T, Nunoi H, Sumimoto H. Novel human homologues of p47phox and p67phox participate in activation of superoxide-producing NADPH oxidases. *J Biol Chem.* 2003;278:25234–25246.
18. Wood SA, Pascoe WS, Schmidt C, Kemler R, Evans MJ, Allen ND. Simple and efficient production of embryonic stem cell-embryo chimeras by coculture. *Proc Natl Acad Sci U S A.* 1993;90:4582–4585.
19. Wassmann S, Stumpf M, Strehlow K, Schmid A, Schieffer B, Bohm M, Nickenig G. Interleukin-6 induces oxidative stress and endothelial dysfunction by overexpression of the angiotensin II type 1 receptor. *Circ Res.* 2004;94:534–541.
20. Daiber A, August M, Baldus S, Wendt M, Oelze M, Sydow K, Kleschyov AL, Munzel T. Measurement of NAD(P)H oxidase-derived superoxide with the luminol analogue L-012. *Free Radic Biol Med.* 2004;36:101–111.

21. Fujiyama S, Amano K, Uehira K, Yoshida M, Nishiwaki Y, Nozawa Y, Jin D, Takai S, Miyazaki M, Egashira K, Imada T, Iwasaka T, Matsubara H. Bone marrow monocyte lineage cells adhere on injured endothelium in a monocyte chemoattractant protein-1–dependent manner and accelerate reendothelialization as endothelial progenitor cells. *Circ Res.* 2003;93:980–989.
22. Katsuyama M, Fan C, Yabe-Nishimura C. NADPH oxidase is involved in prostaglandin F2alpha-induced hypertrophy of vascular smooth muscle cells: induction of NOX1 by PGF2alpha. *J Biol Chem.* 2002;277:13438–13442.
23. Lassegue B, Clempus RE. Vascular NAD(P)H oxidases: specific features, expression, and regulation. *Am J Physiol.* 2003;285:R277–R297.
24. Ortiz MC, Manriquez MC, Romero JC, Juncos LA. Antioxidants block angiotensin II–induced increases in blood pressure and endothelin. *Hypertension.* 2001;38:655–659.
25. Seshiah PN, Weber DS, Rocic P, Valppu L, Taniyama Y, Griendling KK. Angiotensin II stimulation of NAD(P)H oxidase activity: upstream mediators. *Circ Res.* 2002;91:406–413.
26. Chamley-Campbell J, Campbell GR, Ross R. The smooth muscle cell in culture. *Physiol Rev.* 1979;59:1–61.
27. Lusis AJ. *Atherosclerosis Nature.* 2000;407:233–241.
28. Owens GK. Regulation of differentiation of vascular smooth muscle cells. *Physiol Rev.* 1995;75:487–517.
29. Cai H, Harrison DG. Endothelial dysfunction in cardiovascular diseases: the role of oxidant stress. *Circ Res.* 2000;87:840–844.
30. Chabrashvili T, Kitiyakara C, Blau J, Karber A, Aslam S, Welch WJ, Wilcox CS. Effects of ANG II type 1 and 2 receptors on oxidative stress, renal NADPH oxidase, and SOD expression. *Am J Physiol.* 2003;285:R117–R124.

CLINICAL PERSPECTIVE

Involvement of reactive oxygen species (ROSs) generated by membrane-bound NADPH oxidase has been suggested in the pathogenesis of various cardiovascular diseases. NADPH oxidase is a multisubunit enzyme comprising a membrane-associated catalytic subunit (Nox) and several cytosolic regulatory subunits. Among the Nox isoforms recently identified, vascular Nox1 is detected in smooth muscle cells and endothelial cells, whereas Nox2 is localized in endothelial and adventitial cells. A previous report using Nox2-deficient mice demonstrated the involvement of Nox2 in the regulation of the basal blood pressure and in Ang II–induced vascular hypertrophy, but not in the pressor response to Ang II. In this study, Nox1-deficient mice were generated and chronically infused with Ang II. The elevation of blood pressure was significantly blunted compared with wild-type mice, whereas the infusion of pressor as well as subpressor doses of Ang II did elicit marked hypertrophy in the Nox1-deficient aorta. The underlying mechanism of the suppressed pressor response to Ang II was indicated to be the preservation of the availability of nitric oxide through depletion of Nox1-derived ROSs. Nox1/NADPH oxidase, as a downstream unit of Ang II, thus plays a major role in renin-angiotensin system–mediated chronic hypertension. Certainly, roles for NADPH oxidase in ischemic heart disease, cardiac hypertrophy, and arteriosclerosis should be further clarified in Nox-deficient mice. Because each Nox isoform appears to play a distinct role in the development of vascular disorders, isoform-specific inhibitors of the Nox family may become a new generation of therapeutic agents for the treatment of cardiovascular diseases with diverse pathological backgrounds.